

Recent progress on flexible nanogenerators toward self-powered systems

Yiming Liu¹ | Lingyun Wang² | Ling Zhao¹ | Xinge Yu¹ | Yunlong Zi² 

¹Department of Biomedical Engineering, City University of Hong Kong, Hong Kong, People's Republic of China

²Department of Mechanical and Automation Engineering, Chinese University of Hong Kong, Hong Kong, People's Republic of China

Correspondence

Xinge Yu, Department of Biomedical Engineering, City University of Hong Kong, Hong Kong 999077, People's Republic of China.
Email: xingeyu@cityu.edu.hk

Yunlong Zi, Department of Mechanical and Automation Engineering, Chinese University of Hong Kong, Hong Kong 999077, People's Republic of China.
Email: ylzi@cuhk.edu.hk

Funding information

Chinese University of Hong Kong, Grant/Award Number: 4055086; City University of Hong Kong, Grant/Award Number: 9610423; Innovation and Technology Commission, Grant/Award Number: ITS/085/18; Research Grants Council, University Grants Committee, Grant/Award Number: 24206919; Shun Hing Institute of Advanced Engineering, Grant/Award Number: RNE-p5-18

Abstract

The advances in wearable/flexible electronics have triggered tremendous demands for flexible power sources, where flexible nanogenerators, capable of converting mechanical energy into electricity, demonstrate its great potential. Here, recent progress on flexible nanogenerators for mechanical energy harvesting toward self-powered systems, including flexible piezoelectric and triboelectric nanogenerator, is reviewed. The emphasis is mainly on the basic working principle, the newly developed materials and structural design as well as associated typical applications for energy harvesting, sensing, and self-powered systems. In addition, the progress of flexible hybrid nanogenerator in terms of its applications is also highlighted. Finally, the challenges and future perspectives toward flexible self-powered systems are reviewed.

KEYWORDS

flexible systems, hybrid nanogenerator, mechanical energy harvesting, piezoelectric nanogenerator, self-powered system, triboelectric nanogenerator

1 | INTRODUCTION

With the increasing issues of the energy crisis, global warming, and environmental pollution, it is essential to explore renewable energy resources to fulfill the growing demands of the human being to maintain sustainable

development of the society. Green energy sources, including solar, wind, biomass, and hydrogen have been used as alternative energy sources for traditional fossil fuels. Mechanical energy, as another energy form that widely exists in our environment, such as water flow, wind, vibrations, and human motions, is abundant, clean, and sustainable, but usually being wasted in our daily life. Since 2006, the emergence of zinc oxide (ZnO) nanowire-

Yiming Liu and Lingyun Wang contributed equally to this study.

This is an open access article under the terms of the Creative Commons Attribution License, which permits use, distribution and reproduction in any medium, provided the original work is properly cited.

© 2020 The Authors. *InfoMat* published by John Wiley & Sons Australia, Ltd on behalf of UESTC.

based nanogenerator has demonstrated for efficient conversion of mechanical energy into electricity,¹ which has drawn great attention among researchers that various nanogenerators were developed ever since then. With the main focus on mechanical energy harvesting, they are broadly classified into two categories, namely piezoelectric nanogenerator (PENG) and triboelectric nanogenerator (TENG), which are based on their working principles of piezoelectric and triboelectric effects, respectively. Hybrid nanogenerators (HBNG) mainly refer to nanogenerators with the combination of these two and/or other effects such as thermoelectric, pyroelectric, etc.

Nowadays, the blossoming of portable and wearable electronics has triggered the tremendous desires of flexible power sources, where the traditional batteries show limitations of lifespan, disposable issue, and safety problems.² However, the dramatic advances of nanogenerators have demonstrated their promising potential as efficient power supplies for the next-generation electronics, owing to the merits of flexibility, environmentally friendliness, cost-effectiveness, and high output.^{3,4} In the past decades, great efforts have been devoted by researchers to develop nanogenerators with high output and high conversion efficiency from materials' and structures' points of view, with the applications as flexible/wearable power sources toward self-powered systems for various sensing applications.

Here, this review focuses on the recent development of flexible mechanical energy harvesters, including piezoelectric and TENGs through three aspects, namely basic operating mechanisms, materials, and structural designs as well as applications. Besides, HBNGs toward their recent applications are also highlighted. To differentiate from previously published reviews on flexible nanogenerators,^{5,6} this article mainly covers the progress in recent 5 years.

2 | FLEXIBLE PENG

Since the first piezoelectric related work was reported in 1880 by the brothers Pierre Curie and Jacques Curie,⁷ piezoelectric materials have attracted great attentions.⁸⁻¹⁰ The unique properties and exceptional advantages of piezoelectric materials allow broad of applications in the fields of robotics and metrology.¹¹⁻¹³ Recently, soft, and skin-integrated electronics, sometime also known as "epidermal electronics" have been of great interest due to their flexibility, stretchability, and lightweight.¹⁴⁻¹⁷ In the past several years, integration of functional materials into a flexible platform has become a hot research topic.¹⁸⁻²¹ Owing to the advances in materials science and

mechanics, construction of piezoelectric materials in flexible and stretchable formats provides the foundations for numerous applications in wearable and implantable systems.²²⁻²⁵ The piezoelectric coefficient (d_{33}), ratio of open circuit charge density to applied stress (in unit of CN^{-1}), is typically used to quantify the performance of piezoelectric materials. Among the existing piezoelectric materials, lead zirconate titanate (PZT) has been widely applied as the active materials of self-powered electronics for its high d_{33} ($\sim 130 \text{ pmV}^{-1}$).²⁶ However, high lead concentration in PZT renders the fast development of new lead-free piezoelectric materials, such as barium titanate (BaTiO_3), sodium niobite (NaNbO_3), potassium niobite (KNbO_3), and ZnO .^{1,20,27-29} In the past decades, explosive researches and efforts have been devoted to self-powering technologies that convert mechanical energies to electricity. Currently, flexible piezoelectric-based nanogenerators have been recognized as a competitive energy harvesting approach for their high power density output.⁸⁻¹⁰ This section highlights these advances, with an emphasis on operating mechanisms of piezoelectricity, following unusual mechanical attributes and newly developed materials. Various applications derived from those foundations demonstrate the potential of PENG for energy harvesting.

2.1 | Operating mechanisms of piezoelectricity

Piezoelectric materials that convert mechanical deformations to electricity are labeled as a direct piezoelectric effect, while inducing a mechanical strain by an applied electrical field is labeled as converse piezoelectric effect. The piezoelectric effect is governed by the piezoelectric constitutive equation³⁰ as follows:

$$\begin{bmatrix} \delta \\ D \end{bmatrix} = \begin{bmatrix} s^E & d^t \\ d & \epsilon^T \end{bmatrix} \begin{bmatrix} \sigma \\ E \end{bmatrix} \quad (1)$$

where δ and σ represent strain and stress; D and E refer to electric displacement and electric field; s , ϵ , and d are the elastic compliance, the dielectric constant, and the piezoelectric coefficient, respectively; E and T are evaluated at the constant electric field and constant stress, respectively; and t represents the transpose. Originated from the electric dipole moments, piezoelectric effect is partially induced by ions on crystal lattice sites (like ZnO), or by molecular groups directly (like cane sugar).³¹ To clearly describe the operating mechanisms of piezoelectricity, ZnO crystal of wurtzite-structured is selected as an example, as shown in Figure 1.⁸ Figure 1A presents

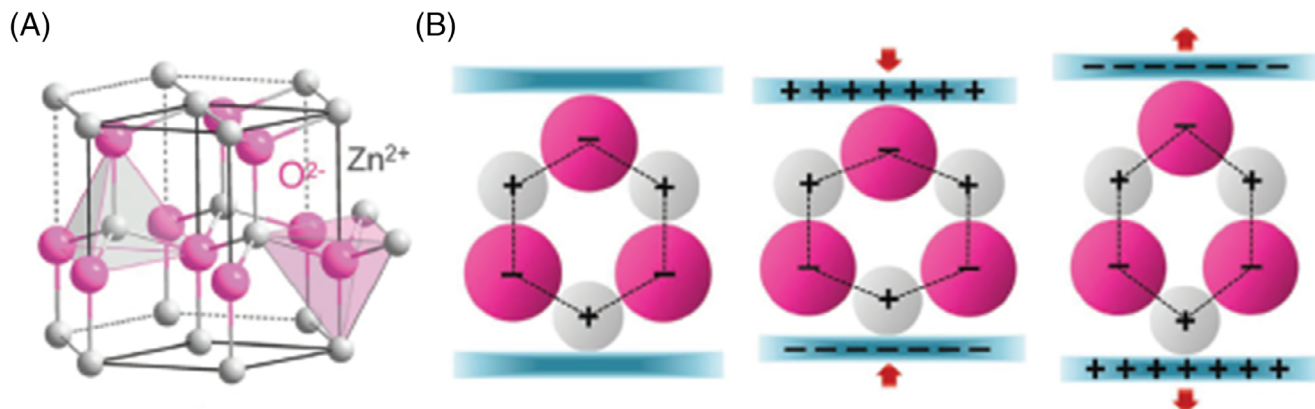


FIGURE 1 Mechanism of ZnO,⁸ Copyright 2017, Wiley-VCH. A, Atomic model of ZnO. B, Working principle of piezoelectric nanogenerator under compression and tension

the tetrahedrally coordinated Zn^{2+} and O^{2-} that accumulate along the *c*-axis. Figure 1B shows the working principle of piezoelectricity induced by ZnO as an external force applied on it. At the initial state, positive and negative charge centers cohere with each other. When an external stress (compressing or stretching) is applied on ZnO, charge centers of anions and cations separate, resulting in an electrical potential, as shown in Figure 1B. The operating mechanism of other widely applied piezoelectric materials can be also explained as mentioned above.

2.2 | Piezoelectric materials and structural design

Since the first report about the piezoelectric material,⁷ many researchers have put remarkable efforts to develop innovative piezoelectric materials, generally being divided into two types, inorganic and organic materials. Compared to the organic piezoelectric materials, inorganic piezoelectric materials exhibit higher piezoelectric constant and coefficient, and thus are widely used for energy harvesting and mechanical sensing. Traditionally, inorganic piezoelectric materials are divided into two parts: piezoelectric crystals and piezoelectric ceramics.^{32–34} Piezoelectric crystal, like ZnO nanowires,³³ have a single crystal structure with natural piezoelectricity. Unlike piezoelectric crystals, piezoelectric ceramics, such as $\text{Ba}(\text{Zr}_x\text{Ti}_{1-x})\text{O}_x$ (BZT)³⁵ and PZT,³⁶ only show piezoelectricity after poling processes, because of their random dipole orientations before poling. However, the brittle and rigid nature of inorganic ceramics limits their applications in flexible electronics. To solve this problem and improve the flexibility and

stretchability, these rigid materials have been developed into thin film, nanowires, nanoparticles, and nanofibers, as shown in Figure 2.^{37–42}

Referring to the deposition method for those piezoelectric thin film or nanocomposite, sol-gel chemistry is no doubt the best route.⁴³ Taking the most used piezoelectric material, PZT for example,^{44–46} precursors of lead, zirconium, and titanium are mixed together and dissolved in solvent. The mixed solution is spin-coated on substrates to form a layer of thin film after hydrolysis, followed up with pre-baking for organic residual removal. To achieve the desired thickness of the film, this process can be repeated multiple times. Eventually a high temperature annealing is performed on the film to form the crystal structures. Besides the solution processing deposition method, physical vapor deposition, for example sputtering, is another deposition method to form thin film of piezoelectric ceramics.⁴⁷ Despite the low-processing temperature of physical vapor deposition compare to sol-gel chemistry, the deposition duration and chamber space restrict the film thickness and film area.⁴⁸ In addition, the physical vapor deposited films usually suffer from poor dielectric constant and coefficients, compared to solution-processed films.⁴⁷ Both organic and inorganic-based piezoelectric materials are able to be formed as nanoscale fibers by particular technique, such as electrospinning. The fiber-based piezoelectric composites show great dipole orientation and separation and therefore afford improved piezoelectric effects.⁴⁹ Meanwhile, the fiber-based piezoelectric materials also show good flexibility under various mechanical strains.⁵⁰ Transfer printing, as a key success to flexible piezoelectric ceramics, involves a liftoff process of the piezoelectric thin film that cast and cured at high temperature on oxidized silicon wafer, where silicon dioxide (SiO_2) serves as

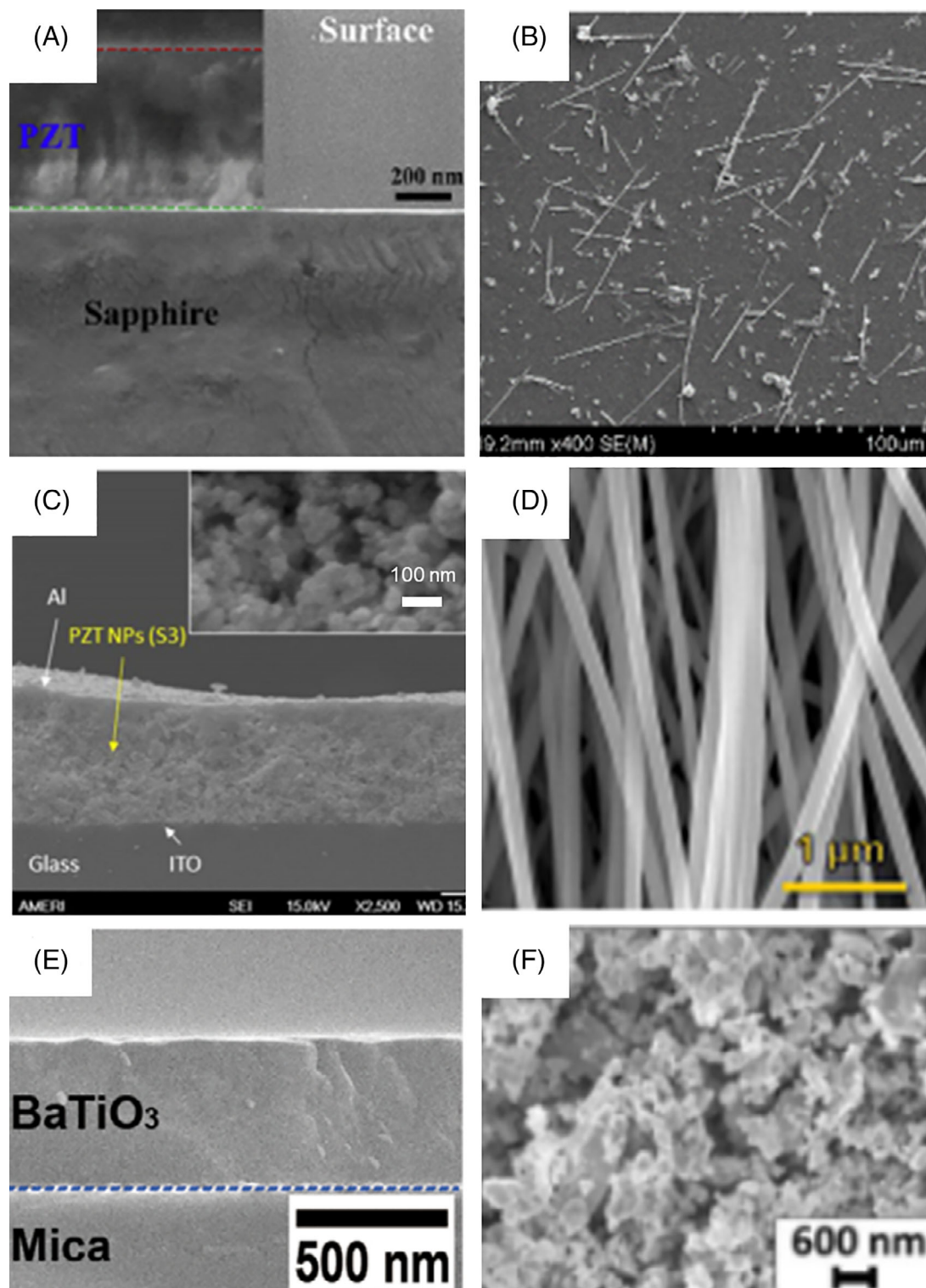


FIGURE 2 Scanning electron microscope (SEM) images of inorganic materials with various structures. Image of (A) PZT thin film,³⁷ Copyright 2019, Elsevier, (B) PZT nanowires,³⁸ Copy 2019, IOP Publishing, (C) PZT nanoparticles,³⁹ Copyright 2016, IOP Publishing, (D) PZT nanofibers,⁴⁰ Copyright 2019, American Chemical Society, (E) BaTiO₃ thin film,⁴¹ Copyright 2019, Wiley-VCH, and (F) BZT nanoparticles,⁴² Copyright 2019, Elsevier

a pre-buried sacrificial layer (removed by chemical wet etching).⁵¹ Another liftoff process of piezoelectric thin films called laser liftoff is associated with exposures to

high energy laser for inducing interface failure between PZT film and sapphire substrate, and thus for transfer printing onto flexible substrates.⁵²

Organic-based piezoelectric materials have been considered as a great candidate flexible electronics due to their inherent flexibility. Polyvinylidene difluoride (PVDF) is the most widely used organic-based piezoelectric material that has five different crystal structures: α , β , δ , γ , and ϵ . The β crystal phase is an electroactive phase which is mainly responsible for piezoelectricity. Therefore, generating stable state of β phase in the polymers can lead to better piezoelectric effect.^{53,54} According to the previous reports, various structures of PVDF and its copolymers have been developed, including fiber arrays, nanowires, thin film, and nanotube arrays.^{55–60} Thin film poly(vinylidene fluoride-co-trifluoroethylene) (P[VDF-TrFE]) owns a significant value for large-area deposition, excellent uniformity, and remarkable surface morphology.⁶¹ However, the piezoelectric constant of the fiber-based composites exhibits about four times greater than the controlled thin film-based ones.⁶² Additionally, PVDF in the format of woven textiles has an exceptional advantage in wearable applications.⁶¹

A key challenge to realize flexible nanogenerator is the development of strategies in mechanics that allows large elastic mechanical deformations and high areal coverages of active devices, even integrating with highly rigid and brittle materials. Therefore, optimizing device structure to enhance the flexibility and power density is desirable. Common piezoelectric-based energy generators adopt sandwich structures, including a functional layer (piezoelectric thin film) with two electrode layers attached at bottom and top,^{44,63,64} as shown in Figure 3A.²⁰ However, the large electrode area limits

mechanical deformations, and thus leads to poor stretchability. To increase the stretchability of the flexible generators, in-plane electrodes can be considered as a great solution. Compared to the sandwich structure, in-plane electrode structure has advantages of thinner thickness, simple fabrication process, and much greater stretchability. Recently, we reported a skin-integrated rubbery electronics with in-plane electrode structure (Figure 3B)⁶⁵ that can survive under various mechanical displacement and rotational boundary condition: stretching up to 15.2%, bending over 160° at a radius of ~30 mm, and twisting 90°. The overall thickness of such generator is less than 1.2 mm, affords great stretchability. Another popular approach involves an island-bridge device design, in which the working area of the electronics at the “islands,” and the electrical interconnects (like serpentine and ribbons) form the “bridges.” Based on the island-bridge layout design, the rigid working areas undertake negligible mechanical deformations whereas the interconnections provide the majority of strain level.²² In-plane mechanical design of electrodes, such as serpentine shape, is another powerful method, which allows the stretchability increases up to hundreds of percentage.⁶⁶

2.3 | Applications

PENGs show the great potential in various fields, ranging from microelectromechanical systems to biomedical engineering. Recently, immense research efforts have been

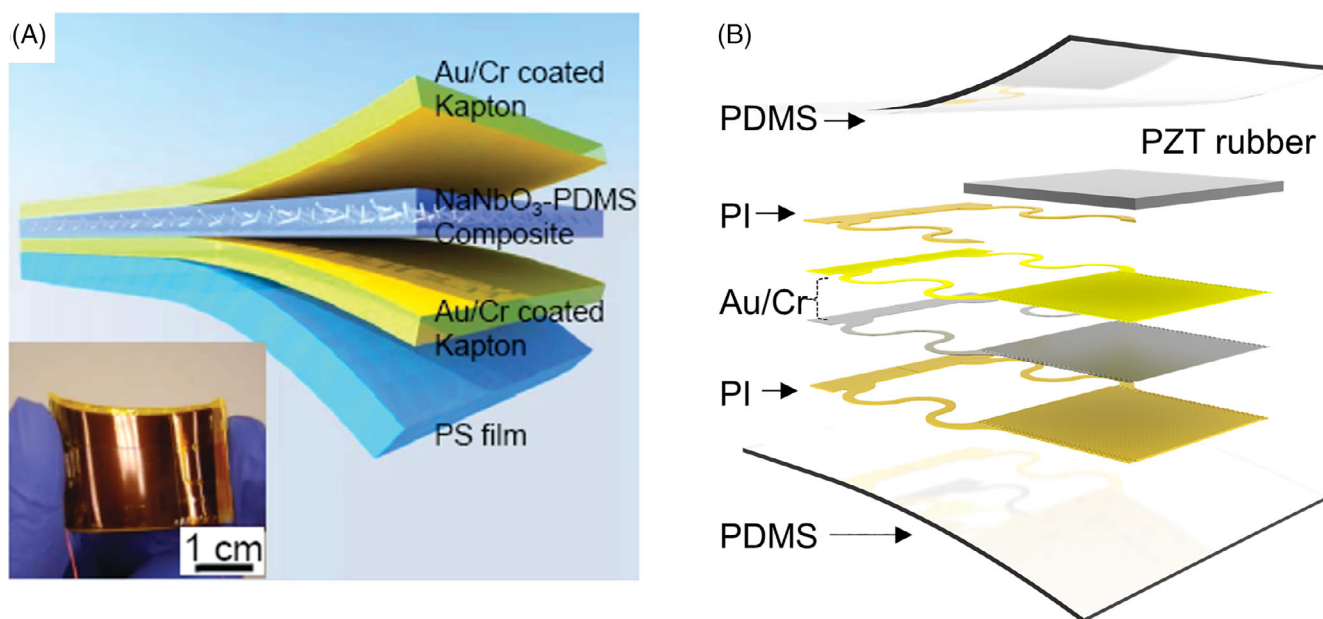


FIGURE 3 Two typical structural designs of PENG, including (A) sandwich structure²⁰ and (B) in-plane electrode structure⁶⁵

made in the application of piezoelectric systems in the biomedical engineering. Rogers's team reported a thin flexible electronics integrating PZT nanoribbons that can be mounted on the surface of internal organs for power generating from mechanical deformations of the organs (Figure 4A).⁶⁷ The energy harvester consisted of multiple PZT nanoribbons connected in series to increase the output voltage. The maximum strain level in these PZT

ribbons is under 0.1% at a bending radius of 2.5 cm, exhibiting excellent flexibility. Owing to the advances in the materials science and engineering, the PZT-based devices exhibit great open-circuit voltage and short-circuit current, and the voltages and currents increase frequency with the same load amplitudes. Output voltage can reach up to ~3.7 V under a strain of 0.35%. The voltage of a micro battery, charged by the device under 7500

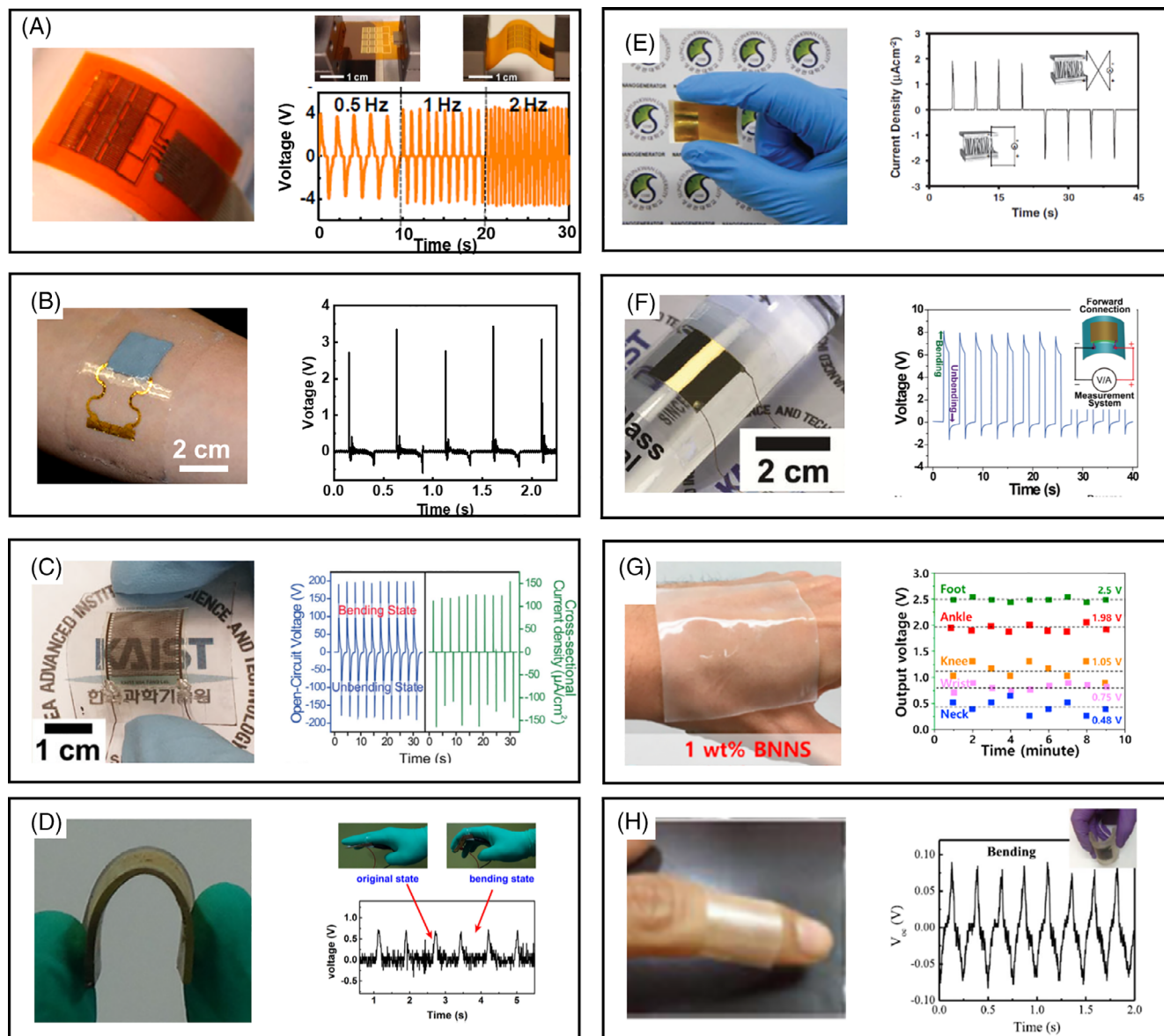


FIGURE 4 Flexible and stretchable piezoelectric nanogenerator applications with various piezoelectric materials. A, Piezoelectric nanogenerator based on PZT nanoribbons,⁶⁷ Copyright 2013, Proceedings of the National Academy of Sciences. B, Skin-integrated piezoelectric nanogenerator based on PZT/PDMS/Graphene composite⁶⁵ Copyright 2019, Wiley-VCH. C, A thin film nanogenerator based on a large-area PZT film on flexible substrates by a laser lift-off process,⁵² Copyright 2014, Wiley-VCH. D, A flexible piezoelectric nanogenerator based on Ag/(K, Na)NbO₃ heterostructure constructed by in-situ photoreduction reaction,⁶⁸ Copyright 2018, Elsevier. E, A thermally stable piezoelectric nanogenerator based on ZnO nanorods,⁶⁹ Copyright 2011, Wiley-VCH. F, A flexible piezoelectric nanogenerator integrating PMN-PT film,⁷⁰ Copyright 2014, Wiley-VCH. G, A piezoelectric nanogenerator incorporating BNNS and PDMS composite,⁷¹ Copyright 2018, Elsevier. H, A Yb³⁺ assisted porous polyvinylidene difluoride (PVDF) composite film comprising flexible piezoelectric nanogenerator,⁷² Copyright 2016, Elsevier

cyclic bending load, saturates at a value of 3.8 V, indicating an electrical energy of ~ 0.164 J. Additionally, the time-averaged power density of five devices can reach as large as $1.2 \mu\text{W cm}^{-2}$, sufficient to power a cardiac pacemaker. Besides the reported PZT-based device, other similar nanogenerators have also been demonstrated to harvest energy from internal organs of animals.⁷³

Recently, we reported a skin-integrated device incorporating PZT/polydimethylsiloxane (PDMS)/graphene composite for mechanical sensing and energy harvesting, as shown in Figure 4B.⁶⁵ Owing to the low elastic modulus of the composite and PDMS (as encapsulation layer), the flexible electronics can stretch up to $\sim 15.2\%$, bend over 160° at a radius of ~ 30 mm, and twist 90° . Moreover, the self-powered nature in the piezoelectric materials allowed energy harvesting from fist striking, with an open-circuit voltage and short-circuit current of 3 V and $1 \mu\text{A}$, respectively. The voltage of 1 nF capacitor, charging by the PZT rubbery device, can reach to 1 V under repeated mechanical beating. To harvest the mechanical energy at human joint areas, the device is mounted onto a wrist, reaching to a maximum voltage of 0.8 V and a current of 58 nA at a bending angle of 15° and a frequency of 4 Hz. As attaching the energy harvester onto a human heel, the device can yield an average voltage and current of 5 V and $52.9 \mu\text{A}$, contributing a remarkable power density of $972.43 \mu\text{W cm}^{-3}$. Besides the PZT rubbery device, there are many nanogenerators based on piezoelectric materials incorporating PDMS, exhibiting excellent ability in harvesting energy from human daily motions.^{20,74,75}

In 2014, Lee et al reported the fabrication of large-area PZT thin films via laser liftoff technique. The commercialized liftoff technique enables a high-quality piezoelectric thin film transfer from bulk sapphire substrates to plastic substrates by XeCl excimer laser. As shown in Figure 4C,⁵² the lightweight and flexible device based on the PZT film yield an open-circuit voltage and short-circuit current of 200 V and $1.5 \mu\text{A}$ under periodical bending and unbending motions with a strain of $\sim 0.386\%$ at a straining rate of $\sim 2.32\% \text{ s}^{-1}$. Moreover, these devices were robust with the test of 9000 bending cycles. As the PZT thin film nanogenerator is connected to an external load resistance ($200 \text{ M}\Omega$), the instantaneous power density reaches up to 17.5 mW cm^{-2} . To further demonstrate the energy conversion from biomechanical movements, a large-area PZT thin film nanogenerator ($5 \times 5 \text{ cm}^2$) can yield a high current of $\sim 8.7 \mu\text{A}$ under irregular and slight bending motions by a human finger. The nanogenerator can directly light up 105 commercial light emitting diode (LED) arrays without rectifier and charge circuit under slightly bending by a human finger. Other PENGs based on an inherently high piezoelectric perovskite thin film

on a plastic substrate are reported.^{26,27,76} Among these attempts, a thin film PENG can output an extremely high power density ($\sim 7 \text{ mW cm}^{-3}$) under periodic mechanical deformations.²⁷

$(\text{Na}_{0.5}\text{K}_{0.5})\text{NbO}_3$ (KNN) is another popular piezoelectric material, due to its high piezoelectric coefficient, large electromechanical coupling factor and good heat stability. Recently, a flexible nanogenerator based on Ag/KNN, multi-walled carbon nanotubes, and PDMS composite was reported by Wang et al (Figure 4D).⁶⁸ Additional conductive materials are introduced to enhance the degree of polarization of the piezoelectric material (KNN), resulting in ultrahigh open-circuit voltage (~ 240 V) and short-circuit current of $\sim 23 \mu\text{A}$ under external mechanical stress of 0.1 MPa. Due to the flexibility of composite layer, the output voltage keeps stable after over 1000 times cycling. Nine white LEDs can be illuminated by the device without any external storage. Figure 3D shows the output performance as the device was deformed by finger bending, an open-circuit voltage of ~ 0.75 V. Under slight foot squeezing, the open-circuit voltage by the device can reach up to ~ 35 V. To further enhance the polarization degree of piezoelectric materials, many researchers attempt to add conductive materials into the piezoelectric composites, like carbon nanotubes.⁷⁷ The nanocomposite generator based on PZT and carbon nanotubes can yield an output voltage and current of ~ 100 V and $\sim 10 \mu\text{A}$, powering 12 commercial LEDs.

ZnO is an excellent candidate for PENG. In 2011, Kim et al reported a ZnO nanorod-based nanogenerator with the first use of cellulose paper as a substrate for its thermal stability, as shown in Figure 4E.⁶⁹ The average diameter and height of ZnO nanorods were 80 nm and $2 \mu\text{m}$, respectively. The output current density was up to $2 \mu\text{A cm}^{-2}$, under the applying external force of 0.8 kgf. Benefited from the thermal stability of cellulose paper, the current output by the device was very stable in a broad temperature range and up to 200°C . To increase the output power density for energy converters, a new single crystalline $(1-x)\text{Pb}(\text{Mg}_{1/3}\text{Nb}_{2/3})\text{O}_3$ - $x\text{PbTiO}_3$ (PMN-PT) has been reported, exhibiting an extremely high piezoelectric charge constant of d_{33} up to 2500 pC N^{-1} (Figure 4F).⁷⁰ Single crystalline rhombohedral PMN-PT ingots were grown directly from the melt by a modified Bridgman method near the morphotropic phase boundary. Periodic bending/unbending motions of the PMN-PT based flexible PENG yielded the output voltage and current of 8.2 V and $145 \mu\text{A}$ ($\sim 411.42 \mu\text{W cm}^{-2}$). Under 30 000 continuous bending cycles at a radius of 16.5 mm, the output current by the device presents negligible degradation, demonstrating its mechanical and electrical stability. Connecting the device to a coin battery through a

rectifier bridge, the voltage of the battery saturates at 1.7 V in 3 hours. As mounting the device on the heart of a rat, the generated energy (2.7 μJ) from the heartbeat is sufficient to trigger the action potential for artificially contracting the heart.

In a recent report, a new piezoelectric material, boron nitride nanotubes (BNNTs), was developed by Sung et al that exhibited excellent electrical, mechanical, and thermal properties (Figure 4G).⁷¹ Benefited from the characteristics of the piezoelectric material, the transparent, flexible, and biocompatible device can be utilized in various applications in energy harvesting. The output voltage and current of the reported generator were 22 V and 75 nA, contributing an output power density of 106 $\mu\text{W cm}^{-3}$ under an external force of 80 kgf. Under 36 000 periodic mechanical beating cycles, the output voltage by the energy harvester still exhibited good stability. Owing to the instinctive nature of the piezoelectric material, the device with a large working area ($7 \times 6.5 \times 0.02 \text{ cm}^3$) was attached to a cellphone display, acting as a touch sensor, and the open-circuit voltage was 4 V under the finger touch. As attached to the different parts of human body, the output voltage can stabilize at 2.5 V for the foot, 1.98 V for the elbow, 0.48 V for the neck, 0.75 V for the wrist, and 1.05 V for the knee under different human movements. Up to now, many reports about the BNNTs have been published, presenting its good high-temperature resistance and piezoelectric capabilities.⁷⁸⁻⁸⁰

PVDF is a typical organic piezoelectric material with inherent flexibility. Many researchers have made much effort to utilize PVDF with various formats in harvesting mechanical energy. It is reported that a PENG based on PVDF nanofibers can yield $\sim 6.5 \mu\text{W}$ with an external resistance load of 5.5 $\text{M}\Omega$.⁸¹ Recently, a PENG based on PVDF that incorporated with hygroscopic rare earth ytterbium salt (Yb-PVDF) was developed by Mandal et al, as shown in Figure 4H.⁷² The device could generate a voltage output of $\sim 85 \text{ mV}$ at continuous bending, and $\sim 70 \text{ mV}$ during repeated twisting. Additionally, the device can produce output voltage of 100–200 mV under the sound pressure ranging from 80 to 100 dB, illustrating its high sensitivity in detecting minuscule stress. As an energy harvester, an open-circuit voltage of $\sim 7 \text{ V}$ was measured by connecting a full wave bridge rectifier during finger imparting (Figure 3H). Connecting the device to an external resistance load ($\sim 20 \text{ M}\Omega$), an instantaneous output power density of $1 \mu\text{W cm}^{-2}$ is achieved, sufficient to power over 50 blue LEDs. More reported PENGs can be found in Table 1.

3 | FLEXIBLE TENG

Triboelectric effect, a contact-induced electrification phenomenon occurs ubiquitously in our daily life, is

normally regarded as a negative effect. Since 2012, the invention of TENG has made full utilization of this effect, converting mechanical energy in the ambient environment into electricity,⁸⁸⁻⁹⁰ such as vibrations,⁹¹⁻⁹³ wind,^{94,95} water waves,^{96,97} and human motions.⁹⁸⁻¹⁰¹ Owing to various advantages of TENG, such as a broad range of material selection, simplicity of structure design, cost-effectiveness, and high output, TENG has been intensively explored in the application of flexible power sources and self-powered environmental sensors, which exhibits the great potential for the future development of wearable electronics and the Internet of Things.¹⁰²⁻¹⁰⁵

3.1 | Operating mechanisms of triboelectricity

Figure 5A demonstrates the construction of the first flexible TENG with vertical contact-separation (CS) mode.⁸⁸ The basic working principle of TENG is through a conjunction of triboelectrification and electrostatic induction, which is illustrated in Figure 5B in detail.⁹³ Generally, a TENG consists of two tribo-materials with different electronegativity, and when the two materials are brought into physical contact, opposite static charges with an equal amount will be generated on the surfaces due to the contact electrification (Figure 5B[II]). Once the two materials are separated, the electrostatic induction induces charges on the two electrodes at the back of two materials (Figure 5B [III]); consequently, a potential difference is established, resulting in electron transfer through the external circuit until an equilibrium state is reached when the two parts are fully separated (Figure 5B [V]). When the two materials approach to each other again, electrons flow in a reverse direction through the external circuit to neutralize the opposite charges on the electrode (Figure 5B [VI]), thus, upon the CS cycles, alternative current signals are generated.

3.2 | Materials and structural design

3.2.1 | Materials

When the two dissimilar tribo-materials are at the two ends of the triboelectric series, higher output is yielded, which is due to the largest difference of electronegativity of these two materials.² Thus, from the material point of view, the electron affinity, surface function groups, as well as work function are important factors affecting the output performance of TENG. A vast number of advanced materials have been explored, including

TABLE 1 Summary of newly developed piezoelectric materials

Materials	Type	d_{33}	Performance	Power density	Reference
ZR5-PNG	Composite	NA	An output voltage of ~85 V and a short-circuit current of ~2.2 μA under repeating bending and relaxation with a frequency of ~4 Hz	$35.62 \mu\text{W cm}^{-2}$	82
Annealed La-doped ZnO-PDMS	Composite	NA	A p-p voltage of 23 V and a p-p current of 150 nA at 2 N force	$1.53 \mu\text{W cm}^{-2}$	83
Li-doped ZnO-PDMS	Composite	~15 pmV^{-1}	The highest output of ~20 V and ~18 $\mu\text{A cm}^{-2}$ under finger bending conditions	5.33 mW cm^{-2}	82
ZnO/Spiro-MeOTAD	Nanowire	NA	An output current density about 500 nA cm^{-2} under vertical compressive force of 1 kgf	N.A.	84
PZT-solid silicon rubber	Composite	NA	The p-p voltage and current of ~65 V and ~1 μA under the aforementioned periodic stretching stimulation.	$\sim 81.25 \mu\text{W cm}^{-3}$	44
PMN-PZT	Film	1527 pC N^{-1}	Open-circuit voltage and short-circuit current of 100 V and 20 μA , respectively, through biomechanical bending and unbending motions	$333.33 \mu\text{W cm}^{-2}$	85
PZT particles-Cu@Ag branch	Nanofibers	NA	The p-p voltage and current of 61 V and 1.1 μA under stretching and releasing deformations (strain of 50%, strain rate of 6.4 cm s^{-1} and frequency of 0.7 Hz)	$22.36 \mu\text{W cm}^{-3}$	84
KNN-BTO-PDMS	Composite	NA	An electrical output of 58 V and 450 nA	$2.9 \mu\text{W cm}^{-2}$	75
PVDF-KNN	Composite	NA	An electrical output of 3.7 V and 0.326 μA	N.A.	86
PVDF-MAPbI ₃	Composite	NA	An electrical output of 17.8 V and 2.1 $\mu\text{A cm}^{-2}$ under an applied mechanical force 50 N	$37.38 \mu\text{W cm}^{-2}$	87
P(VDF-TrFE)-BNNTs	Composite	14 pC N^{-1}	The output voltage and current of 22 V and 640 nA and a sensitivity of 55 V/MPa under the pressure of 0.4 MPa	$11.3 \mu\text{W cm}^{-2}$	18
BSFTO-PDMS	Composite	18 pC N^{-1}	An electrical output of 16 V and 2.8 μA under the vertical force of 35 N	$3.11 \mu\text{W cm}^{-2}$	19

graphene,¹⁰⁶⁻¹⁰⁹ MXenes,^{110,111} hydrogels,¹¹²⁻¹¹⁵ aerogels,¹¹⁶⁻¹¹⁸ black phosphorus (BP),¹¹⁹ etc.

Due to the uniqueness of mechanical flexibility, chemical stability, and high electron mobility, graphene has been regarded as a promising candidate for energy-related applications. Recently, a crumpled graphene (CG)-based TENG was reported as shown in Figure 6A.¹⁰⁸ The CG layer was formed on pre-strained VHB tape (3M, VHB 4910), endowing its high stretchability and flexibility. The output performance of the device was enhanced with the increase of the crumple degree, which is ascribed to the increased contact area, surface roughness, and larger work function difference. Another graphene-based stretchable TENG is reported as a self-powered touch sensor with an overall thickness around 18 μm (Figure 6B). It can conformally contact on the uneven surface of the human palm and the sensitivity was 0.274 V kPa^{-1} in the pressure range of 1~40 kPa.¹⁰⁹

MXenes, a recently emerging family of two-dimensional materials, whose electrical and mechanical properties can be tuned by adjusting the composition and surface functional groups such as $-\text{O}$, $-\text{OH}$, and $-\text{F}$, was found more tribo-negative than polytetrafluoroethylene (PTFE).¹¹⁰ Dong et al reported that a layer of MXenes ($\text{Ti}_3\text{C}_2\text{T}_x$) film fabricated by spray coating its aqueous suspension on glass had a neutral state when contacting against PTFE, while a voltage of 650 V can be delivered when contacted with polyethylene terephthalate (PET) (Figure 6C). This is mainly because $\text{Ti}_3\text{C}_2\text{T}_x$ has the same terminal groups with PTFE.¹¹⁰ Flexible TENG can be realized by coating the MXenes on flexible substrates, such as ITO/PET. Furthermore, an all electrospun TENG was fabricated comprising poly(vinyl alcohol) (PVA) and $\text{Ti}_3\text{C}_2\text{T}_x$ composite nanofiber film and silk nanofibers film, which can output 1087 mW m^{-2} power density.¹²⁰

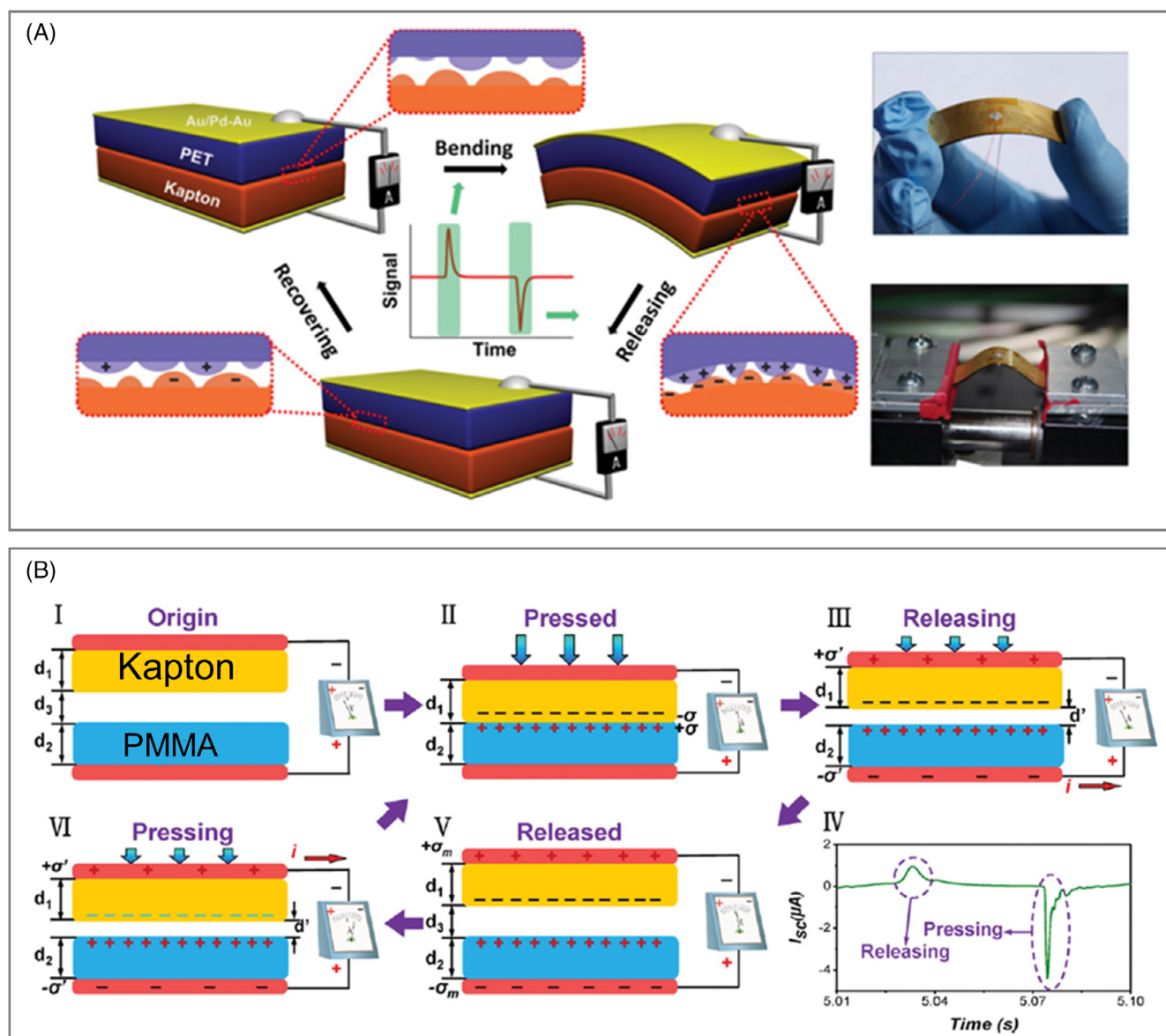


FIGURE 5 Construction and working principle of the first flexible triboelectric nanogenerator (TENG). A, The construction and digital photos of the flexible TENG.⁸⁸ Copyright 2012, Elsevier. B, Working principle of the flexible TENG.⁹³ Copyright 2012, American Chemical Society

Recently, hydrogels as ideal ionic conductors have been widely studied as efficient current collectors in TENG applications. For example, Wang et al reported hydrogels with hybrid electronic/ionic conductivity consisting of silver nanowires and chitosan (CS) cross-linked by metal ions (Ag^+/Cu^{2+}) as current collectors for harvesting human motion energy (Figure 6D).¹¹⁵ The output performance of the TENG was associated with the concentration of silver nanowires as well as the complexation type of metal ions. In addition, ionogel-based TENG was also reported with a wider application temperature range ($-20^\circ C \sim 100^\circ C$) comparing to that of hydrogel-based.¹²¹ Moreover, cross-linked polyethyleneimide

(PEI)/PVA was developed by researchers as positive tribo-materials, and the composite-based TENG shows a much higher output when embedding Au nanoparticles in the polymer matrix, which was due to a 2.4-fold enhancement of dielectric constant of the composite bulk.¹²²

Due to the highly porous structures and super lightweight, aerogels have been developed in various applications. Mi et al reported a cellulose nanofibrils/PEI porous aerogel serving as positive material and in contact with PVDF in TENG¹¹⁷ as shown in Figure 6E. The output power density of the device improved 14.4 times due to the enhanced tribo-positivity. In addition, other materials

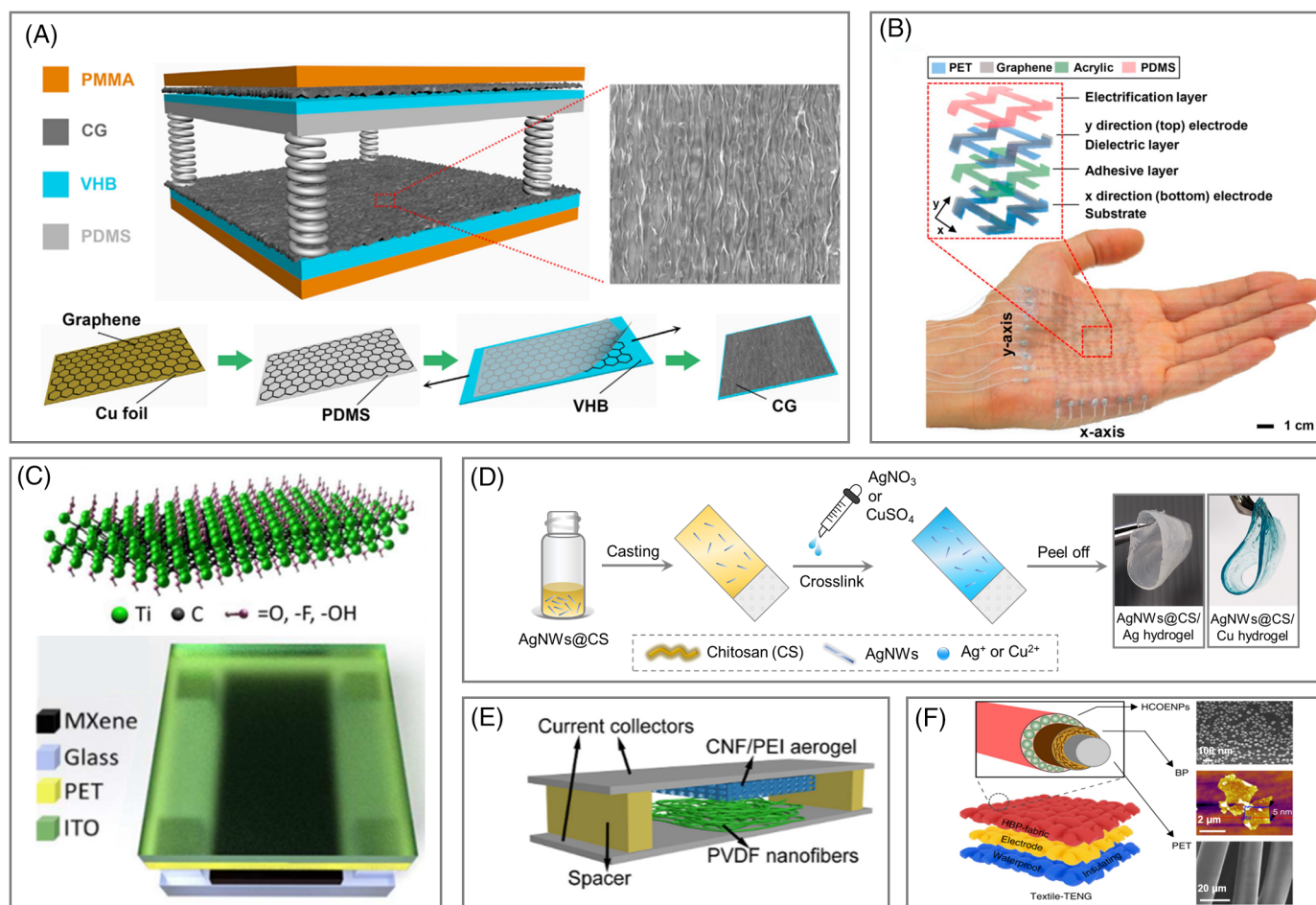


FIGURE 6 Material choices for the triboelectric nanogenerator (TENG). A, Crumpled graphene (CG)-based TENG.¹⁰⁸ Copyright 2019, Elsevier. B, Graphene as electrode.¹⁰⁹ Copyright 2019, Elsevier. C, MXenes-based TENG.¹¹⁰ Copyright 2018, Elsevier. D, Chitosan (CS)-based hydrogel as electrode.¹¹⁵ Copyright 2019, Elsevier. E, Cellulose nanofibril/polyethyleneimide (CNF/PEI) aerogel-based TENG.¹¹⁷ Copyright 2018, Elsevier. F, Modified textile-based TENG¹¹⁹

are also reported as the various choices of tribo-materials or electrodes for TENG application. For example, cashmere-based TENG,¹²³ modified textile-based TENG by BP, and cellulose-derived hydrophobic nanoparticles (Figure 6F),¹¹⁹ wrinkled PEDOT: PSS film,¹²⁴ ultrathin paper-based self-powered system,¹²⁵ patterned Ag nanofiber electrodes,¹²⁶ and so forth. A summary of the output characteristics of TENGs based on various materials was listed in Table 2.

3.2.2 | Structural design

Basically, TENG has four working modes, including CS mode, lateral sliding mode, single-electrode (SE) mode, and sliding freestanding triboelectric-layer (SFT) mode.³ The basic structure for all these four working modes composes at least one pair of triboelectric surfaces as well

as two electrodes. For SFT mode, there are two pairs of triboelectric surfaces and the ground serves as the other electrode for SE mode.¹⁰³ A lot of structures have been designed in line with these four modes. Here, we mainly review the representative structures of each working mode.

The CS mode is vastly been studied due to its simple structure, easy fabrication, and high instantaneous power density. Surface functionalization,^{133,134} micro/nano-structure patterning,^{135,136} and bulk property engineering^{137,138} of the tribo-materials are frequently adopted by researchers to improve the output power. In the meantime, a lot of new designs have emerged. Figure 7A shows an ultraflexible three-dimensional TENG (3D-TENG) fabricated by hybrid 3D printing technique.¹³⁹ This 3D-TENG uses printed resin composites as the tribo-electrification layer and ionic hydrogel as electrodes. Each unit undergoes CS cycles when the entire structure

TABLE 2 Summary of output characteristics of triboelectric nanogenerators (TENGs) with different triboelectric materials

Materials	Working mode	Open-circuit voltage and short-circuit current (density)	Power density	Reference
Crumpled graphene	CS	Contact against PDMS, 83 V, 25.78 μA	2.5 W m^{-2}	108
$\text{Ti}_3\text{C}_2\text{T}_x$	CS	Contact against paper, ~ 119 V, ~ 22 μA	~ 609.1 mW m^{-2}	111
Au/PEI/PVA	CS	Contact against PET, 161.1 V, 20 mAm^{-2}	17.73 W m^{-2}	122
Porous CTS/PI aerogel	CS	Contact against porous PDMS, 60.6 V, 7.7 μA	2.33 W m^{-2}	116
Paper	CS	Contact against FEP, 90 V, 6 mAm^{-2}	285.6 mW m^{-2}	125
Textile modified with black phosphorus	SE	Contact against skin, ~ 1860 V, 1.1 $\mu\text{A cm}^{-2}$	5.2 W m^{-2}	119
Zeolitic imidazole framework (ZIF)	CS	Contact against Kapton, 164 V, 7 μA	392 mW m^{-2}	127
Nylon	CS	Contact against silicone rubber, 1.17 kV, 138 μA	11.2 W m^{-2}	128
Polyacrylonitrile/polyamide 6	CS	Contact against PVDF/PDMS, 540 V, 110 μA	14.8 W m^{-2}	129
BNO-sulfonated polyimide	CS	Contact against PTFE, 75 V, 1 μA	178.5 mW m^{-2}	130
Polytetrafluoroethylene foam	CS	Contact against PTFE, 12 V, 8.5 nA	NA	131
Graphene oxide	SE	Contact against skin, 1100 V, 55 μA	3.13 W m^{-2}	132

is deformed and released by an external force. Also, it is found that the output performance is associated with compression ratio, the structure, and parameters (D , d) of the unit. A higher compression ratio enhances the effective contact surface area, endowing the increase of electrostatic charges per unit volume. Besides, the increase of D and d in each unit largely decreases the distance h , which results in decreased output voltage while the output current and power are in an opposite trend, owing to the improvement of effective contact area. This 3D-TENG can produce a peak power per unit volume of 10.98 W m^{-3} under a low frequency of 1.3 Hz. Similarly, knitted fabric/textile-based TENGs usually adopt the CS mode.^{144,145}

Recently, an interesting snow-based TENG was developed for harvesting energy in harsh snowy environment with triboelectrification of snow as shown in Figure 7B.¹⁴⁰ They used a 3D printing technique for the triboelectric layer of silicone and the electrode of poly (3,4-ethylene dioxythiophene)-poly (styrene sulfonate) (PEDOT: PSS) in a single electrode mode. The snow, as crystallized water, carries positive charges and will have contact electrification with silicone when falling or sliding on the surface of silicone. Consequently, the device generates an instantaneous power density of 0.2 mW m^{-2} . Besides, the device shows the potential application as an arctic weather station for measurement of various meteorological parameters, including snowfall rate/direction, wind speed, and snow depth. Similar structures

are frequently employed for wind energy and rain-drop energy harvesting.¹⁴⁶

TENGs with SFT structure can harvest energy from moving objects while the system can still mobile without grounding wires,¹⁴⁷ which is suitable for harvesting rotating motion energy, human walking, and air flow, etc. Guo et al reported a TENG consisting of checker-like interdigital metal electrodes (aluminum [Al]) and a sandwiched PET film, which can convert translational kinetic energy in all directions¹⁴¹ as shown in Figure 7C. When the PTFE squares and acrylic of the sliding pane move in certain direction, electricity is generated upon the separation and contact. The sandwiched PET film between the sliding panel and metal electrodes can be worn freely, thus, the operation lifetime of the device is greatly increased. The resultant TENG can yield an open-circuit voltage of 210 V in the X or Y sliding direction, a maximum output power density of 1.9 W m^{-2} and has the advantages of light weight, durable, flexible to fold, and portable.

To further enhance the output performance, various stacked-layer TENGs are proposed. Figure 7D shows a concept of electrical muscle stimulation powered by a zigzag TENG. In this TENG, a PET layer is firstly folded in a zigzag structure and Al layers are stacked to each surface of the folded PET layer as electrodes. PTFE serving as a triboelectric layer against Al film is assembled on top of another counterpart Al film. Finally, the stacked TENG is wrapped by another PET layer to confine the

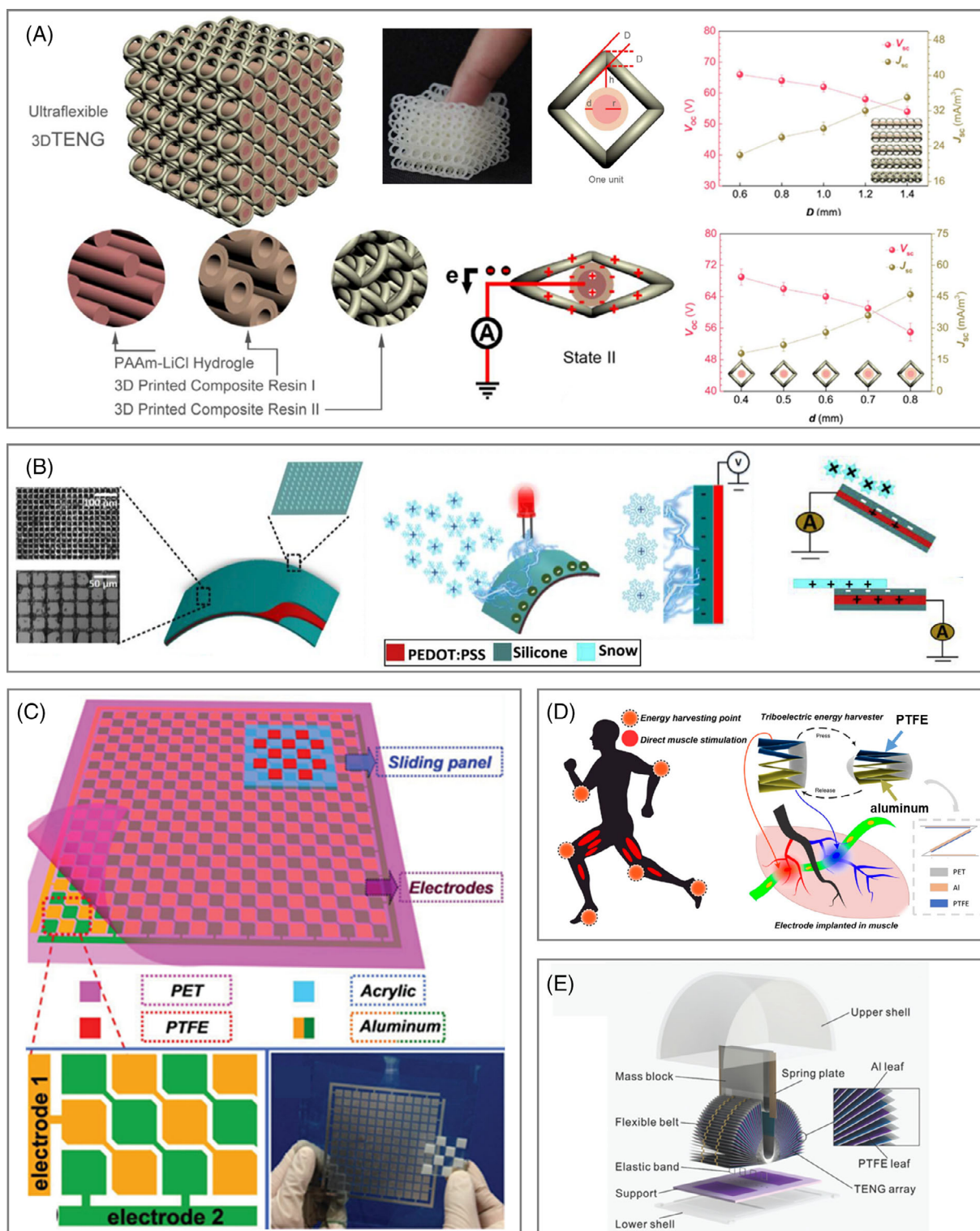


FIGURE 7 Representative and novel structures of triboelectric nanogenerator (TENG). A, Three-dimensional (3D) structured TENG.¹³⁹ Copyright 2018, Elsevier. B, Snow-based TENG with a single-electrode structure.¹⁴⁰ Copyright 2019, Elsevier. C, Sliding freestanding triboelectric-layer (SFT) structured TENG with checker-like electrodes.¹⁴¹ Copyright 2015, Wiley-VCH. D, Zig-zag structured TENG.¹⁴² Copyright 2019, American Chemical Society. E, Open-book-like TENG.¹⁴³ Copyright 2019, Royal Society of Chemistry

structure.¹⁴² Thus, during pressing and releasing operation, the zigzag TENG can automatically return to the original position before next pressing and the mechanical

deformation energy is converted to electricity with a short-circuit current of 35 μ A. In addition, another stacked TENG with the open-book-like structure is reported

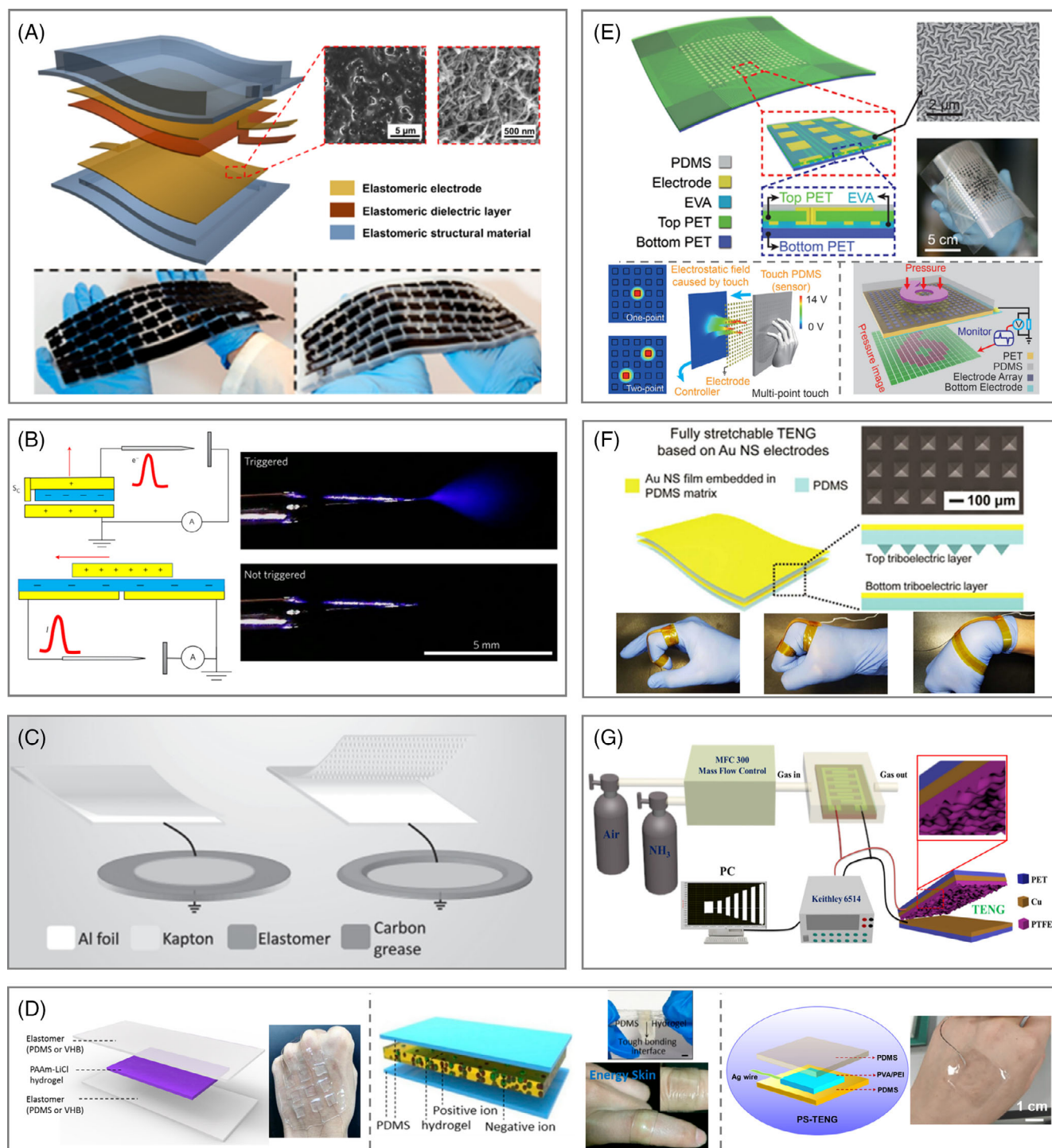


FIGURE 8 Various applications of flexible triboelectric nanogenerator (TEG). A, TENG-based keyboard cover as a power supply through harvesting typing energy.¹⁵⁵ Copyright 2016, American Chemical Society. B, TENG driving nano-coulomb molecular mass spectrometry.¹⁴⁹ Copyright 2017, Springer Nature. C, TENG driving dielectric elastomer actuator.¹⁵⁰ Copyright 2016, Wiley-VCH. D, TENG-based E-skins.^{113,114,151} Copyright 2017, The American Association for the Advancement of Science. Copyright 2018, American Chemical Society. Copyright 2019, Wiley-VCH. E TENG-based sensor for real-time tactile mapping.¹⁵³ Copyright 2016, Wiley-VCH. F, TENG-based sensor for human motion detection.¹⁵² Copyright 2017, Elsevier. G, TENG-based sensor for NH_3 gas sensing.¹⁵⁴ Copyright 2018, Elsevier

by Zhong et al as shown in Figure 7E. The device can integrate multiple TENG units in a limited space and greatly enhanced the volume density. For a device

with 50-unit TENG, the transferred charges and the short-circuit current are 26 μC and 0.45 mA, respectively.¹⁴³

3.3 | Applications

Ever since the invention of TENG, it has been vastly explored as efficient power sources by scavenging different types of mechanical energy in the ambient environment and as self-powered sensors for various sensing applications. Comprehensive reviews about applications of TENG have been published.¹⁴⁸ In this section, some representative examples will be reviewed including driving different actuators,^{149,150} TENG-based E-skin,^{113,114,151} motion detector,¹⁵² tactile mapping,¹⁵³ chemical sensors,¹⁵⁴ and so on.

Conventionally, biomechanical energy such as typing or pressing buttons is wasted in our daily life, Li et al developed an all-elastomer TENG-based keyboard cover for typing energy harvesting,¹⁵⁵ as shown in Figure 8A. The keyboard cover consists of five elastomer layers, including structural elastomer (two layers), carbon black and carbon nanotubes-based elastomeric electrodes (two layers), and elastomeric dielectric layer (one layer). Through the optimization of material and structural aspects, the cover shows a high transferred charge density of $140 \mu\text{C m}^{-2}$. Furthermore, the fully packaged keyboard was integrated with a supercapacitor as a self-powered system. Continuously typing the keyboard for 1 hour under normal speed, around 0.8 mJ of electricity can be stored to drive an electronic thermometer. This TENG-based keyboard cover successfully demonstrates the conversion of typing energy into electricity and is useful to further research the typing behavior of different people.

Since the high output voltage characteristics of TENG, it has been employed by researchers to drive various kinds of actuators. Recently, Li et al reported a novel application of TENG for sensitive nano-coulomb molecular mass spectrometry,¹⁴⁹ as shown in Figure 8B. In this system, the total amount of ionization charges in mass spectrometry can be quantitatively regulated by the output of TENG. The authors show that plasma discharge ionization and nanoelectrospray ionization (nanoESI) are successfully induced by single-polarity or alternating-polarity ion pulses, which are generated by the high output voltage of two modes of TENG. This system opens a door for quantitative and highly sensitive mass spectrometric analysis using charge amount as well as demonstrates a facile and effective approach of TENG-driven ionization.

In addition, another application of high output voltage of TENG is for driving dielectric elastomer actuator (DEA) as reported by Chen et al (Figure 8C).¹⁵⁰ Dielectric elastomers are similar with human skins in terms of low elastic modulus and large strain capability.¹⁵⁶ Besides, they are actuator materials and their deformation can be

controlled by an external high voltage. In this work, the authors delivered a self-powered actuation system composing of a SE TENG and a DEA. When the TENG (100 cm^2) working at a CS velocity of $0.1\text{--}10 \text{ cm s}^{-1}$, an expansion strain of 14.5% can be induced for the DEA device with electrode diameter of 0.6 cm. The findings show its promising applications in artificial muscles and soft electronics.

Recently, soft skin-like TENGs with multiple functionalities such as high transparency and flexibility/stretchability for biomechanical energy harvesting and sensing received great interest among researchers. Figure 8D exhibits three examples of TENG-based E-skins with a sandwich structure composed of two elastomers (PDMS/VHB) and one layer of ionic hydrogel. The first skin-like TENG reported by Pu et al shows an ultra-high stretchability (1160%) and high transparency (96.2% in visible-light range).¹¹³ This device can yield an open-circuit voltage of 145 V and a peak power density of 35 mW m^{-2} . Meanwhile, the E-skin sensing pressure as low as 1.3 kPa was demonstrated. Due to the easy dehydration of hydrogels, toughly bonded elastomer/hydrogel hybrids through interfacial modification to ensure the stable mechanical and electrical performance of the E-skin device was reported by Liu et al.¹¹⁴ After the tough interfacial bonding, the dehydration of the hybrids is greatly alleviated with an average dehydration decreases by over 73%. Furthermore, Wang et al reported a transparent and flexible polyionic-skin TENG (PS-TENG) with resistance to dehydration.¹⁵¹ The output of the PS-TENG shows no significant degradation after storage in a desiccator under vacuum (RH of 23% at 23.8°C) for 5 days. Besides, the device demonstrates the output characteristics under tapping, bending, and curling.

Alternatively, another TENG-based E-skin toward practical applications of human-machine interfaces was developed by Wang et al¹⁵³ as shown in Figure 7E. In this work, a flexible self-powered high-resolution (5 dpi) triboelectric sensor matrices (TESM) with 16×16 pixels based on a SE mode TENG is implemented, which can real-time map single-point and multi-point tactile stimuli with a remarkable pressure sensitivity of 0.06 kPa^{-1} . PDMS serving as electrification layer in TESM was dry-etched to micro/nanostructure morphology to enhance the effective contact area. Besides, the side length of each pixel is 2.5 mm and more precise tactile sensing can be realized by reducing the pixel size to micron-size level. The study demonstrates the capabilities of the large-scale potential application of real-time triboelectric tactile mapping in touch sensing, motion tracking, and human-machine interfaces.

To overcome the deterioration of TENG-based human-motion detection performance, which may be

induced by repeated stretching/releasing cycles with mechanical fracture, a stretchable and durable self-powered human-motion detector was reported by Lim et al (Figure 8F).¹⁵² Au nanosheet (NS)-embedded PDMS was employed as electrode and bottom triboelectric layer with patterned PDMS serving as the counter tribo-layer. This Au NS-TENG-based sensor was demonstrated for index finger, knuckle, and wrist bending and relaxation motion detection, demonstrating good bendability, stretchability, and durability.

Lastly, TENG-based chemical sensors are explored for different chemical sensing applications. Figure 8G shows an ultrasensitive flexible self-powered NH_3 sensor based on polyaniline-multiwalled carbon nanotubes (PANI-MWCNTS) composite thin film driven by a CS mode TENG.¹⁵⁴ It is found that the output of NH_3 sensor has a

proportional correlation with the concentration of NH_3 . This gas sensing system shows a response of 10% at a low concentration of NH_3 (0.001 ppm) and 225% at a higher concentration (100 ppm). Besides, the practical sensing application is extended to testing the human exhaled NH_3 . This study shows the potential application of TENG-based self-powered chemical sensor for environmental detector and human kidney health sensing.

4 | FLEXIBLE HBNG

Piezoelectric and triboelectric HBNGs are widely utilized to convert raw energies into usable electricity. TENGs transform mechanical energy to electricity by a coupling effect of triboelectrification and electrostatic induction,

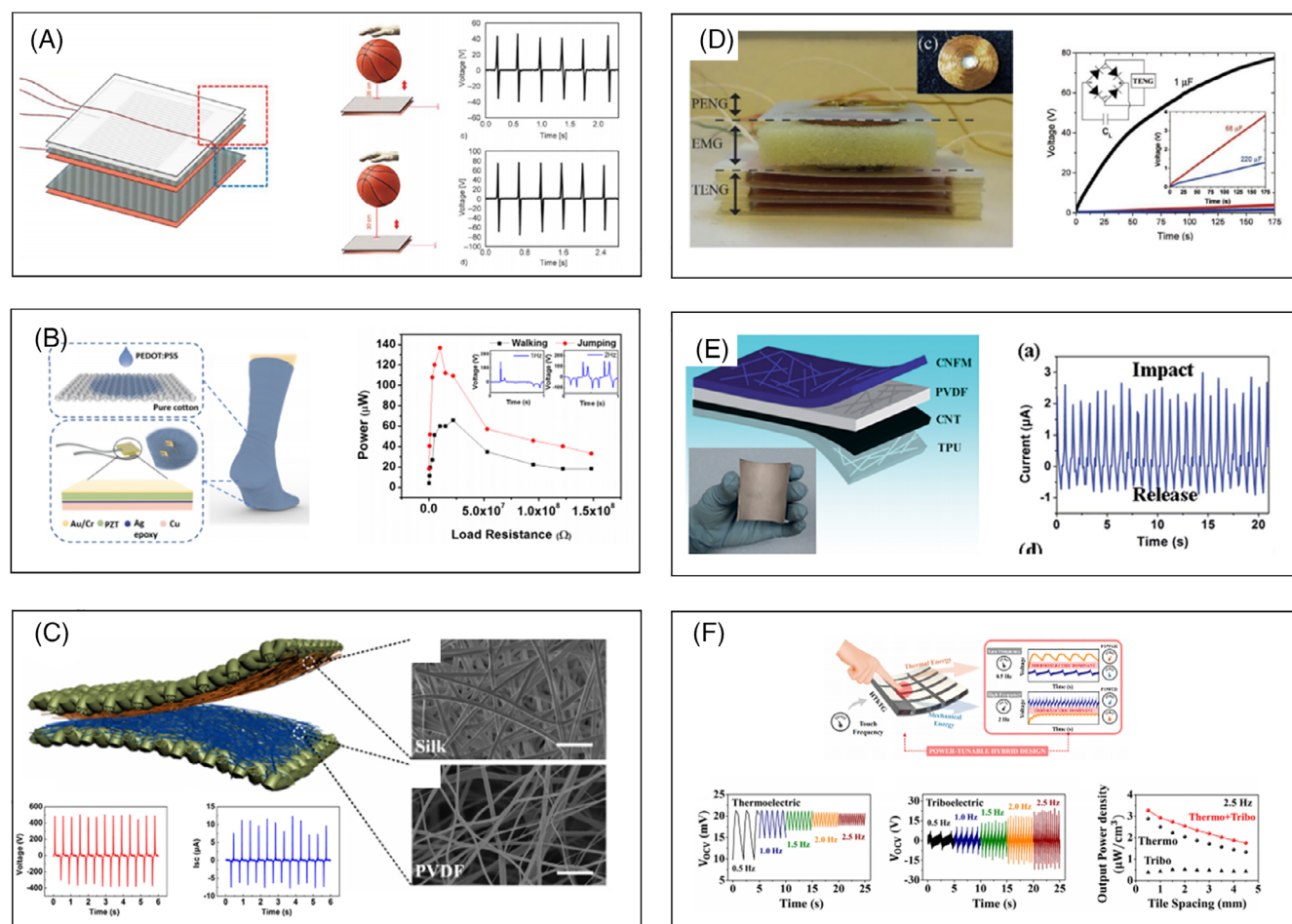


FIGURE 9 Flexible hybrid nanogenerators with various materials. A, A hybrid piezoelectric-triboelectric nanogenerator using polyvinylidene difluoride (PVDF) as the functional layer of piezoelectric nanogenerator,¹⁶¹ Copyright 2019, ProQuest. B, A self-powered sock based on PEDOT:PSS coated triboelectric nanogenerator and PZT piezoelectric nanogenerator,¹⁶⁰ Copyright 2019, American Chemical Society. C, A hybrid tribo-piezo nanogenerator based on PVDF nanofibers and silk fibroin nanofibers,¹⁶² Copyright 2018, Elsevier. D, A flexible hybrid triboelectric-electromagnetic-piezoelectric nanogenerator,¹⁶³ Copyright 2019, Elsevier. E, A hybrid pyroelectric-piezoelectric nanogenerator incorporating PVDF,¹⁶⁴ Copyright 2018, Royal Society of Chemistry. F, A thermal-triboelectric generator consisting of bismuth telluride tiles with PDMS,¹⁶⁵ Copyright 2019, American Chemical Society

while PENGs convert mechanical energy to electricity by electric dipole movements. To maximize the energy conversion efficiency, a concept of HBNGs has been built up that associates with the combination of various mechanisms of electromagnetics, electrostriction, pyroelectricity, piezoelectricity, and triboelectricity. For example, hybrid tribo-piezo nanogenerators can yield great electrical power derived from both triboelectric and piezoelectric effects at the same time.¹⁵⁷ Although the electromagnetic-based generators are widely applied in daily life, the HBNGs involving electromagnetic effect are relatively bulk due to their intrinsic operation mechanism.¹⁵⁸⁻¹⁶⁰

Herein, we review the recent works of flexible HBNGs and their applications. As shown in Figure 9A, a fully encapsulated piezoelectric-triboelectric HBNG was reported by Fuh et al, where organic piezoelectric thin film PVDF was used as the piezoelectric functional layer and the copper and printed circuit board were adopted as the triboelectric functional layers.¹⁶¹ This hybrid generator could yield an output voltage of ~130 V and a current of 4 μ A under hands-induced mechanical deformation. The authors applied the HBNG in sports for detecting different basketball dribbling heights (Figure 9A). Figure 8B presents a self-powered sock that consisted of poly(3,4-ethylenedioxythiophene) polystyrenesulfonate (PEDOT: PSS) coated TENGs and PZT PENGs.¹⁶⁶ By tuning the external loading resistances, the output power of the sock could be boosted up to 66 and 137 μ W under 1 Hz walking and 2 Hz jumping. Combining the power generated from the PTFE based "shoe pad," the maximum power output of 1.71 mW was obtained. Another advanced wearable generator is based on textile materials, which can serve as cloth and harvest energy from the daily human motions. Figure 9C shows a textile-based hybrid tribo-piezo nanogenerator which was made of silk fibroin and PVDF nanofibers.¹⁶² Under hand tapping and folding, the textile HBNG afforded a great power output (500 V, 12 μ A). After working for 10 000 cycles at 2 Hz, no cracks can be observed from scanning electron microscope images, demonstrating its mechanical durability.

Compared to the typical hybrid triboelectric-PENGs, triboelectric-electromagnetic-PENGs obtain less attentions due to their relatively bulk volume derived from complicated configurations. A representative triboelectric-electromagnetic PENG reported by Ventura et al¹⁶³ made some efforts on the device design to improve the flexibility and output power. The resulted HBNG composed of three separated parts, a PENG (ZnO nanowires) on the top, an electromagnetic nanogenerator (planar coil and magnet) in the middle, and a TENG (Nylon 6.6 and PTFE) at the bottom (Figure 9D). The

maximum open-circuit voltage of ~75 V and short-circuit current of ~45 mA were obtained, which could be used for charging capacitors. To scavenge mechanical and thermal energies, flexible HBNGs based on piezoelectric (or triboelectric) and pyroelectric effects is also discussed here. In 2018, Long et al reported a flexible pyroelectric-piezoelectric HBNG that adopted thermoplastic polyurethane nanofiber membrane-carbon nanotubes composites as pyroelectric materials and substrates, electrospun PVDF nanofiber membrane as piezoelectric functional layer, and an electrospun poly(3,4-ethylenedioxythiophene):poly(styrenesulfonate)-polyvinyl pyrrolidone conductive nanofiber membrane (PEDOT:PSS-PVP) as electrodes (Figure 9E).¹⁶⁴ The device was able to harvest energy from the human daily motions, yielding a short-current as high as 320 nA. Recently, Choi et al reported a tribo-pyro HBNG that used bismuth telluride and PDMS as the pyroelectric and triboelectric functional materials (Figure 9F).¹⁶⁵ The n-type and p-type are connected by series. Therefore, as heat is delivered to the device by finger touching, electrons from n-type and holes of p-type will be driven to the cold side, generating current in the circuit. Meanwhile, an electrical potential was generated on PDMS and skin due to the triboelectric effect. This nanogenerator could effectively work under lower frequency (<5 Hz), and afforded a maximum power density of 3.27 μ W cm⁻³.

5 | CONCLUSION AND PERSPECTIVE

In summary, we systematically summarize the recent progress of flexible piezoelectric and TENGs in terms of their basic working principles, materials and structural designs, and applications. Furthermore, recent development of HBNGs is also reviewed. Since the invention of piezoelectric and TENGs, substantial efforts have been devoted to enhance the output performance of the two types of nanogenerators, achieving several orders of magnitude enhancement. The advances of flexible mechanical energy harvesters have already demonstrated the great potential in the next-generation electronics. It can be anticipated that more significance will be achieved by further development of this technology and dramatic impact will be received not only on the future progress of flexible electronics but also on our daily lives.

Nevertheless, some research aspects need to be considered toward further development of flexible nanogenerators and more work should be done in tackling the potential issues and constraints. First, with more new materials developed for mechanical energy harvesting

applications, the fundamental understanding of the mechanism in terms of charge transfer will benefit the optimization of the output characteristics to maximize the energy conversion efficiency. The impact of environmental conditions on the output performance is one of the key factors that are required to be considered in order to fully understand the working mechanism. Second, in addition to flexibility, novel structural design with multifunctionalities, such as stretchability, transparency, durability, degradability, and so on, are highly desirable to meet the different working scenarios toward real applications. Besides, consideration of the effective package of the device cannot be neglected to implement an efficient flexible power source. Finally, fully integration of the flexible power sources with other flexible/wearable electronics to realize self-powered systems relies on efficient power-management systems as well as energy-storage devices.

ACKNOWLEDGMENTS

This work is supported by HKSAR The Research Grants Council Early Career Scheme (Grant no. 24206919), HKSAR Innovation and Technology Support Programme Tier 3 (Grant no. ITS/085/18), The Chinese University of Hong Kong Direct Grant (Grant no. 4055086), Shun Hing Institute of Advanced Engineering (Grant no. RNE-p5-18), and City University of Hong Kong (Grant No. 9610423).

CONFLICT OF INTEREST

The authors declare no conflict of interest.

ORCID

Yunlong Zi  <https://orcid.org/0000-0002-5133-4057>

REFERENCE

- Wang ZL, Song JH. Piezoelectric nanogenerators based on zinc oxide nanowire arrays. *Science*. 2006;312(5771):242-246.
- Wang ZL. Triboelectric nanogenerators as new energy technology for self-powered systems and as active mechanical and chemical sensors. *ACS Nano*. 2013;7(11):9533-9557.
- Wang ZL, Chen J, Lin L. Progress in triboelectric nanogenerators as a new energy technology and self-powered sensors. *Energy Environ Sci*. 2015;8(8):2250-2282.
- Wu C, Wang AC, Ding W, Guo H, Wang ZL. Triboelectric nanogenerator: a foundation of the energy for the new era. *Adv Energy Mater*. 2019;9(1):1802906.
- Fan FR, Tang W, Wang ZL. Flexible nanogenerators for energy harvesting and self-powered electronics. *Adv Mater*. 2016;28(22):4283-4305.
- Wang Y, Yang Y, Wang ZL. Triboelectric nanogenerators as flexible power sources. *npj Flexible Electr*. 2017;1(1):10.
- Curie J, Curie P. Développement par compression de l'électricité polaire dans les cristaux hémihédres à faces inclinées. *Bull Minéral*. 1880;3(4):90-93.

- Zheng Q, Shi B, Li Z, Wang ZL. Recent progress on piezoelectric and triboelectric energy harvesters in biomedical systems. *Adv Sci*. 2017;4(7):1700029.
- Liu H, Zhong J, Lee C, Lee S-W, Lin L. A comprehensive review on piezoelectric energy harvesting technology: materials, mechanisms, and applications. *Appl Phys Rev* 2018;5(4):041306. <https://doi.org/10.1063/1.5074184>.
- Dagdeviren C, Joe P, Tuzman OL, et al. Recent progress in flexible and stretchable piezoelectric devices for mechanical energy harvesting, sensing and actuation. *Extreme Mech Lett*. 2016;9:269-281.
- Seminara L, Capurro M, Cirillo P, Cannata G, Valle M. Electromechanical characterization of piezoelectric PVDF polymer films for tactile sensors in robotics applications. *Sens Actuator A: Phys*. 2011;169(1):49-58.
- Kolesar ES, Dyson CS. Object imaging with a piezoelectric robotic tactile sensor. *J Microelectromech Syst*. 1995;4(2):87-96.
- Dürselen R, Grunewald U, Preuss W. Calibration and applications of a high-precision piezo scanner for nanometrology. *Scanning*. 1995;17(2):91-96.
- Huang S, Liu Y, Zhao Y, Ren Z, Guo CF. Flexible electronics: stretchable electrodes and their future. *Adv Funct Mater*. 2019;29(6):1805924.
- Hong YJ, Jeong H, Cho KW, Lu N, Kim DH. Wearable and implantable devices for cardiovascular healthcare: from monitoring to therapy based on flexible and stretchable electronics. *Adv Funct Mater*. 2019;29(19):1808247.
- Dong K, Peng X, Wang ZL. Fiber/fabric-based piezoelectric and triboelectric nanogenerators for flexible/stretchable and wearable electronics and artificial intelligence. *Adv Mater*. 2019;1902549. <https://doi.org/10.1002/adma.201902549>.
- Yu X, Xie Z, Yu Y, et al. Skin-integrated wireless haptic interfaces for virtual and augmented reality. *Nature*. 2019;575(7783):473-479.
- Ye S, Cheng C, Chen X, et al. High-performance piezoelectric nanogenerator based on microstructured P (VDF-TrFE)/BNNTs composite for energy harvesting and radiation protection in space. *Nano Energy*. 2019;60:701-714.
- Zhang Y, Wu M, Zhu Q, et al. Performance enhancement of flexible piezoelectric nanogenerator via doping and rational 3D structure design for self-powered mechanosensational system. *Adv Funct Mater*. 2019;29:1904259.
- Jung JH, Lee M, Hong J-I, et al. Lead-free NaNbO₃ nanowires for a high output piezoelectric nanogenerator. *ACS Nano*. 2011;5(12):10041-10046.
- Hou S, Yu J, Zhuang X, et al. Phase separation of P3HT/PMMA blend film formed semiconducting and dielectric layers in organic thin-film transistors for high sensitivity NO₂ detection. *ACS Appl Mater Interfaces*. 2019;11:44521-44527.
- Zhang Y, Wang S, Li X, et al. Experimental and theoretical studies of serpentine microstructures bonded to prestrained elastomers for stretchable electronics. *Adv Funct Mater*. 2014;24(14):2028-2037.
- Li J, Chen S, Liu W, et al. High performance piezoelectric based on electrospun ZnO nanorods/poly (vinylidene fluoride) composite membranes. *J Phys Chem C*. 2019;123(18):11378-11387.
- Su Y, Ping X, Yu KJ, et al. In-plane deformation mechanics for highly stretchable electronics. *Adv Mater*. 2017;29(8):1604989.

25. Lu B, Chen Y, Ou D, et al. Ultra-flexible piezoelectric devices integrated with heart to harvest the biomechanical energy. *Sci Rep*. 2015;5:16065.
26. Qi Y, Kim J, Nguyen TD, Lisko B, Purohit PK, McAlpine MC. Enhanced piezoelectricity and stretchability in energy harvesting devices fabricated from buckled PZT ribbons. *Nano Lett*. 2011;11(3):1331-1336.
27. Park K-I, Xu S, Liu Y, et al. Piezoelectric BaTiO₃ thin film nanogenerator on plastic substrates. *Nano Lett*. 2010;10(12):4939-4943.
28. Cauda V, Stassi S, Bejtka K, Canavese G. Nanoconfinement: an effective way to enhance PVDF piezoelectric properties. *ACS Appl Mater Interfaces*. 2013;5(13):6430-6437.
29. Yang Y, Jung JH, Yun BK, et al. Flexible pyroelectric nanogenerators using a composite structure of lead-free KNbO₃ nanowires. *Adv Mater*. 2012;24(39):5357-5362.
30. Erturk A, Inman DJ. *Piezoelectric Energy Harvesting*. Chichester: John Wiley & Sons; 2011.
31. Bharathkumar M, Yellappa P, Revanth D. A novel pliant nanogenerator made of PDMS and ZnO nanoparticles. *i-Manager's J Electr Eng*. 2015;5(3):30-34.
32. Mattiat OE. *Ultrasonic Transducer Materials*. New York: Springer Science & Business Media; 1917.
33. Anton SR, Sodano HA. A review of power harvesting using piezoelectric materials (2003–2006). *Smart Mater Struct*. 2007;16(3):R1-R21.
34. Kim HS, Kim J-H, Kim J. A review of piezoelectric energy harvesting based on vibration. *Int J Precis Eng Manuf*. 2011;12(6):1129-1141.
35. Li B, Blendell JE, Bowman KJ. Temperature-dependent poling behavior of lead-free BZT-BCT piezoelectrics. *J Am Ceram Soc*. 2011;94(10):3192-3194.
36. Chaipanich A, Jaitanong N, Tunkasiri T. Fabrication and properties of PZT-ordinary Portland cement composites. *Mater Lett*. 2007;61(30):5206-5208.
37. He J, Zhang J, Qian S, et al. Flexible heterogeneous integration of PZT film by controlled spalling technology. *J Alloys Compd*. 2019;807:151696.
38. Pang L, Zhao Q, Sheng T, et al. Enhanced pressure & proximity sensitivities of a flexible transparent capacitive sensor with PZT nanowires. Paper presented at: IOP Conference Series: Materials Science and Engineering; 2019.
39. Paik YH, Kojori HS, Kim SJ. Ferroelectric devices using lead zirconate titanate (PZT) nanoparticles. *Nanotechnology*. 2016;27(7):075204.
40. Lee H, Kim H, Kim DY, Seo Y. Pure piezoelectricity generation by a flexible nanogenerator based on lead zirconate titanate nanofibers. *ACS Omega*. 2019;4(2):2610-2617.
41. Hyeon DY, Park K-I. Piezoelectric flexible energy harvester based on BaTiO₃ thin film enabled by exfoliating the mica substrate. *Energ Technol*. 2019;7:1900638.
42. Shin D-J, Ji J-H, Kim J, Jo GH, Jeong S-J, Koh J-H. Enhanced flexible piezoelectric energy harvesters based on BaZrTiO₃-BaCaTiO₃ nanoparticles/PVDF composite films with Cu floating electrodes. *J Alloys Compd*. 2019;802:562-572.
43. Yu X, Marks TJ, Facchetti A. Metal oxides for optoelectronic applications. *Nat Mater*. 2016;15(4):383-396.
44. Niu X, Jia W, Qian S, et al. High-performance PZT-based stretchable piezoelectric nanogenerator. *ACS Sustain Chem Eng*. 2018;7(1):979-985.
45. Chen X, Xu S, Yao N, Shi Y. 1.6 V nanogenerator for mechanical energy harvesting using PZT nanofibers. *Nano Lett*. 2010;10(6):2133-2137.
46. Babu I, de With G. Highly flexible piezoelectric 0–3 PZT-PDMS composites with high filler content. *Compos Sci Technol*. 2014;91:91-97.
47. Pandey S, James A, Prakash C, Goel T, Zimik K. Electrical properties of PZT thin films grown by sol-gel and PLD using a seed layer. *Mater Sci Eng B*. 2004;112(1):96-100.
48. Zheng X, Li J, Zhou Y. X-ray diffraction measurement of residual stress in PZT thin films prepared by pulsed laser deposition. *Acta Mater*. 2004;52(11):3313-3322.
49. Chen X, Xu S, Yao N, Xu W, Shi Y. Potential measurement from a single lead zirconate titanate nanofiber using a nanomanipulator. *Appl Phys Lett*. 2009;94(25):253113.
50. Qi Y, McAlpine MC. Nanotechnology-enabled flexible and biocompatible energy harvesting. *Energ Environ Sci*. 2010;3(9):1275-1285.
51. Meitl MA, Zhu Z-T, Kumar V, et al. Transfer printing by kinetic control of adhesion to an elastomeric stamp. *Nat Mater*. 2006;5(1):33-38.
52. Park KI, Son JH, Hwang GT, et al. Highly-efficient, flexible piezoelectric PZT thin film nanogenerator on plastic substrates. *Adv Mater*. 2014;26(16):2514-2520.
53. Lim C, He L. Exact solution of a compositionally graded piezoelectric layer under uniform stretch, bending and twisting. *Int J Mech Sci*. 2001;43(11):2479-2492.
54. Zhang X-J, Wang G-S, Wei Y-Z, Guo L, Cao M-S. Polymer-composite with high dielectric constant and enhanced absorption properties based on graphene-CuS nanocomposites and polyvinylidene fluoride. *J Mater Chem A*. 2013;1(39):12115-12122.
55. Yao P, Zhu B, Zhai H, et al. PVDF/Palygorskite nanowire composite electrolyte for 4 V rechargeable lithium batteries with high energy density. *Nano Lett*. 2018;18(10):6113-6120.
56. Fujitsuka N, Sakata J, Miyachi Y, et al. Monolithic pyroelectric infrared image sensor using PVDF thin film. *Sens Actuators A: Phys*. 1998;66(1–3):237-243.
57. Chen X, Shao J, Li X, Tian H. A flexible piezoelectric-pyroelectric hybrid nanogenerator based on P (VDF-TrFE) nanowire array. *IEEE Trans Nanotechnol*. 2016;15(2):295-302.
58. Park YJ, Kang SJ, Park C, et al. Irreversible extinction of ferroelectric polarization in P (VDF-TrFE) thin films upon melting and recrystallization. *Appl Phys Lett*. 2006;88(24):242908.
59. Li X, Lim Y-F, Yao K, Tay FEH, Seah KH. P (VDF-TrFE) ferroelectric nanotube array for high energy density capacitor applications. *Phys Chem Chem Phys*. 2013;15(2):515-520.
60. Sümer B, Aksak B, Şahin K, Chuengsatansup K, Sitti M. Piezoelectric polymer fiber arrays for tactile sensing applications. *Sens Lett*. 2011;9(2):457-463.
61. Sharma T, Je S-S, Gill B, Zhang JX. Patterning piezoelectric thin film PVDF-TrFE based pressure sensor for catheter application. *Sens Actuators A: Phys*. 2012;177:87-92.
62. Soin N, Shah TH, Anand SC, et al. Novel “3-D spacer” all fibre piezoelectric textiles for energy harvesting applications. *Energ Environ Sci*. 2014;7(5):1670-1679.

63. Sun J, Yang A, Zhao C, Liu F, Li Z. Recent progress of nanogenerators acting as biomedical sensors in vivo. *Sci Bull.* 2019; 64:1336-1347.
64. Lin Z-H, Yang Y, Wu JM, Liu Y, Zhang F, Wang ZL. BaTiO₃ nanotubes-based flexible and transparent nanogenerators. *J Phys Chem Lett.* 2012;3(23):3599-3604.
65. Liu Y, Zhao L, Wang L, et al. Skin-integrated graphene-embedded lead zirconate titanate rubber for energy harvesting and mechanical sensing. *Adv Mater Technol.* 2019;4(12): 1900744.
66. Kim DH, Liu Z, Kim YS, et al. Optimized structural designs for stretchable silicon integrated circuits. *Small.* 2009;5(24): 2841-2847.
67. Dagdeviren C, Yang BD, Su Y, et al. Conformal piezoelectric energy harvesting and storage from motions of the heart, lung, and diaphragm. *Proc Natl Acad Sci USA.* 2014;111(5):1927-1932.
68. Huan Y, Zhang X, Song J, et al. High-performance piezoelectric composite nanogenerator based on Ag/(K, Na) NbO₃ heterostructure. *Nano Energy.* 2018;50:62-69.
69. Kim KH, Lee KY, Seo JS, Kumar B, Kim SW. Paper-based piezoelectric nanogenerators with high thermal stability. *Small.* 2011;7(18):2577-2580.
70. Hwang GT, Park H, Lee JH, et al. Self-powered cardiac pacemaker enabled by flexible single crystalline PMN-PT piezoelectric energy harvester. *Adv Mater.* 2014;26(28): 4880-4887.
71. Kim K-B, Jang W, Cho JY, et al. Transparent and flexible piezoelectric sensor for detecting human movement with a boron nitride nanosheet (BNNS). *Nano Energy.* 2018;54:91-98.
72. Ghosh SK, Biswas A, Sen S, et al. Yb³⁺ assisted self-polarized PVDF based ferroelectric nanogenerator: a facile strategy of highly efficient mechanical energy harvester fabrication. *Nano Energy.* 2016;30:621-629.
73. Li Z, Zhu G, Yang R, Wang AC, Wang ZL. Muscle-driven in vivo nanogenerator. *Adv Mater.* 2010;22(23):2534-2537.
74. Jung JH, Chen C-Y, Yun BK, et al. Lead-free KNbO₃ ferroelectric nanorod based flexible nanogenerators and capacitors. *Nanotechnology.* 2012;23(37):375401.
75. Vivekananthan V, Chandrasekhar A, Alluri NR, et al. A flexible piezoelectric composite nanogenerator based on doping enhanced lead-free nanoparticles. *Mater Lett.* 2019;249:73-76.
76. Qi Y, Jafferis NT, Lyons K Jr, Lee CM, Ahmad H, McAlpine MC. Piezoelectric ribbons printed onto rubber for flexible energy conversion. *Nano Lett.* 2010;10(2):524-528.
77. Park KI, Jeong CK, Ryu J, Hwang GT, Lee KJ. Flexible and large-area nanocomposite generators based on lead zirconate titanate particles and carbon nanotubes. *Adv Energy Mater.* 2013;3(12):1539-1544.
78. Suryavanshi AP, Yu M-F, Wen J, Tang C, Bando Y. Elastic modulus and resonance behavior of boron nitride nanotubes. *Appl Phys Lett.* 2004;84(14):2527-2529.
79. Kang JH, Sauti G, Park C, et al. Multifunctional electroactive nanocomposites based on piezoelectric boron nitride nanotubes. *ACS Nano.* 2015;9(12):11942-11950.
80. Blase X, Rubio A, Louie S, Cohen M. Stability and band gap constancy of boron nitride nanotubes. *EPL.* 1994;28(5):335-340.
81. Yu L, Zhou P, Wu D, Wang L, Lin L, Sun D. Shoe pad nanogenerator based on electrospun PVDF nanofibers. *Microsyst Technol.* 2019;25(8):3151-3156.
82. He S, Guo Y, Guo R, Fu X, Guan L, Liu H. Piezoelectric nanogenerators based on self-poled two-dimensional Li-doped ZnO microdisks. *J Electr Mater.* 2019;48(5):2886-2894.
83. Rajagopalan P, Khandelwal G, Palani I, Singh V, Kim S-J. La-doped ZnO ultra-flexible flutter-piezoelectric nanogenerator for energy harvesting and sensing applications: a novel renewable source of energy. *Nanoscale.* 2019;11:14032-14041.
84. Zhu J, Qian J, Hou X, et al. High-performance stretchable PZT particles/Cu@ Ag branch nanofibers composite piezoelectric nanogenerator for self-powered body motion monitoring. *Smart Mater Struct.* 2019;28(9):095014.
85. Hwang GT, Yang J, Yang SH, et al. A reconfigurable rectified flexible energy harvester via solid-state single crystal grown PMN-PZT. *Adv Energy Mater.* 2015;5(10):1500051.
86. Bairagi S, Ali SW. A unique piezoelectric nanogenerator composed of melt-spun PVDF/KNN nanorod-based nanocomposite fibre. *Eur Polym J.* 2019;116:554-561.
87. Jella V, Ippili S, Eom J-H, Choi J, Yoon S-G. Enhanced output performance of a flexible piezoelectric energy harvester based on stable MAPbI₃-PVDF composite films. *Nano Energy.* 2018; 53:46-56.
88. Fan FR, Tian ZQ, Wang ZL. Flexible triboelectric generator! *Nano Energy.* 2012;1(2):328-334.
89. Shi Q, He T, Lee C. More than energy harvesting—combining triboelectric nanogenerator and flexible electronics technology for enabling novel micro-nano-systems. *Nano Energy.* 2019;57:851-871.
90. Lee KY, Chun J, Lee J-H, et al. Hydrophobic sponge structure-based triboelectric nanogenerator. *Adv Mater.* 2014; 26(29):5037-5042.
91. Xiao X, Zhang XA, Wang SY, et al. Honeycomb structure inspired triboelectric nanogenerator for highly effective vibration energy harvesting and self-powered engine condition monitoring. *Adv Energy Mater.* 2019;9:1902460.
92. Wu CS, Liu RY, Wang J, Zi YL, Lin L, Wang ZL. A spring-based resonance coupling for hugely enhancing the performance of triboelectric nanogenerators for harvesting low-frequency vibration energy. *Nano Energy.* 2017;32:287-293.
93. Zhu G, Pan C, Guo W, et al. Triboelectric-generator-driven pulse electrodeposition for micropatterning. *Nano Lett.* 2012; 12(9):4960-4965.
94. Zhao ZF, Pu X, Du CH, et al. Freestanding flag-type triboelectric nanogenerator for harvesting high-altitude wind energy from arbitrary directions. *ACS Nano.* 2016;10(2):1780-1787.
95. Chen B, Yang Y, Wang ZL. Scavenging wind energy by triboelectric nanogenerators. *Adv Energy Mater.* 2018;8(10): 1702649.
96. Zhao XJ, Kuang SY, Wang ZL, Zhu G. Highly adaptive solid-liquid interfacing triboelectric nanogenerator for harvesting diverse water wave energy. *ACS Nano.* 2018;12(5):4280-4285.
97. Xu L, Jiang T, Lin P, et al. Coupled triboelectric nanogenerator networks for efficient water wave energy harvesting. *ACS Nano.* 2018;12(2):1849-1858.
98. Zhang ZX, Du K, Chen X, Xue CY, Wang KY. An air-cushion triboelectric nanogenerator integrated with stretchable electrode for human-motion energy harvesting and monitoring. *Nano Energy.* 2018;53:108-115.
99. Xia KQ, Zhu ZY, Zhang HZ, Du CL, Fu JM, Xu ZW. Milk-based triboelectric nanogenerator on paper for harvesting

- energy from human body motion. *Nano Energy*. 2019;56:400-410.
100. Cui C, Wang X, Yi Z, et al. Flexible single-electrode triboelectric nanogenerator and body moving sensor based on porous Na_2CO_3 /polydimethylsiloxane film. *ACS Appl Mater Interfaces*. 2018;10(4):3652-3659.
101. Meng B, Tang W, Too Z-h, et al. A transparent single-friction-surface triboelectric generator and self-powered touch sensor. *Energ Environ Sci*. 2013;6(11):3235-3240.
102. Zhu G, Peng B, Chen J, Jing QS, Wang ZL. Triboelectric nanogenerators as a new energy technology: from fundamentals, devices, to applications. *Nano Energy*. 2015;14:126-138.
103. Zi YL, Wang ZL. Nanogenerators: an emerging technology towards nanoenergy. *APL Mater*. 2017;5(7):074103.
104. Chen L, Shi Q, Sun Y, Nguyen T, Lee C, Soh S. Controlling surface charge generated by contact electrification: strategies and applications. *Adv Mater*. 2018;30(47):1802405.
105. Liu Y, Wang L, Zhao L, et al. Thin, skin-integrated, stretchable triboelectric nanogenerators for tactile sensing. *Adv Electr Mater*. 2019;1901174. <https://doi.org/10.1002/aelm.201901174>.
106. Stanford MG, Li JT, Chyan Y, Wang Z, Wang W, Tour JM. Laser-induced graphene triboelectric nanogenerators. *ACS Nano*. 2019;13(6):7166-7174.
107. Parandeh S, Kharaziha M, Karimzadeh F. An eco-friendly triboelectric hybrid nanogenerators based on graphene oxide incorporated polycaprolactone fibers and cellulose paper. *Nano Energy*. 2019;59:412-421.
108. Chen HM, Xu Y, Zhang JS, Wu WT, Song GF. Enhanced stretchable graphene-based triboelectric nanogenerator via control of surface nanostructure. *Nano Energy*. 2019;58:304-311.
109. Lee Y, Kim J, Jang B, et al. Graphene-based stretchable/wearable self-powered touch sensor. *Nano Energy*. 2019;62:259-267.
110. Dong YC, Mallineni SSK, Maleski K, et al. Metallic MXenes: a new family of materials for flexible triboelectric nanogenerators. *Nano Energy*. 2018;44:103-110.
111. Jiang C, Li X, Yao Y, et al. A multifunctional and highly flexible triboelectric nanogenerator based on MXene-enabled porous film integrated with laser-induced graphene electrode. *Nano Energy*. 2019;66:104121.
112. Lee Y, Cha SH, Kim YW, Choi D, Sun JY. Transparent and attachable ionic communicators based on self-cleanable triboelectric nanogenerators. *Nat Commun*. 2018;9:1804.
113. Pu X, Liu MM, Chen XY, et al. Ultrastretchable, transparent triboelectric nanogenerator as electronic skin for biomechanical energy harvesting and tactile sensing. *Sci Adv*. 2017;3(5):e1700015.
114. Liu T, Liu MM, Dou S, et al. Triboelectric-nanogenerator-based soft energy-harvesting skin enabled by toughly bonded elastomer/hydrogel hybrids. *ACS Nano*. 2018;12(3):2818-2826.
115. Wang L, Daoud WA. Hybrid conductive hydrogels for washable human motion energy harvester and self-powered temperature-stress dual sensor. *Nano Energy*. 2019;66:104080.
116. Zheng QF, Fang LM, Guo HQ, et al. Highly porous polymer aerogel film-based triboelectric nanogenerators. *Adv Funct Mater*. 2018;28(13):1706365.
117. Mi HY, Jing X, Zheng QF, et al. High-performance flexible triboelectric nanogenerator based on porous aerogels and electrospun nanofibers for energy harvesting and sensitive self-powered sensing. *Nano Energy*. 2018;48:327-336.
118. Qian ZC, Li R, Guo J, et al. Triboelectric nanogenerators made of polybenzazole aerogels as fire-resistant negative tribo-materials. *Nano Energy*. 2019;64:103900.
119. Xiong JQ, Cui P, Chen XL, et al. Skin-touch-actuated textile-based triboelectric nanogenerator with black phosphorus for durable biomechanical energy harvesting. *Nat Commun*. 2018;9:4280.
120. Jiang CM, Wu C, Li XJ, et al. All-electrospun flexible triboelectric nanogenerator based on metallic MXene nanosheets. *Nano Energy*. 2019;59:268-276.
121. Sun LJ, Chen S, Guo YF, et al. Ionogel-based, highly stretchable, transparent, durable triboelectric nanogenerators for energy harvesting and motion sensing over a wide temperature range. *Nano Energy*. 2019;63:103847.
122. Wang LY, Yang XY, Daoud WA. High power-output mechanical energy harvester based on flexible and transparent Au nanoparticle-embedded polymer matrix. *Nano Energy*. 2019;55:433-440.
123. Wang LY, Yang XY, Daoud WA. Mechanical energy harvester based on cashmere fibers. *J Mater Chem A*. 2018;6(24):11198-11204.
124. Wen Z, Yang YQ, Sun N, et al. A wrinkled PEDOT:PSS film based stretchable and transparent triboelectric nanogenerator for wearable energy harvesters and active motion sensors. *Adv Funct Mater*. 2018;28(37):1803684.
125. He X, Zi YL, Yu H, et al. An ultrathin paper-based self-powered system for portable electronics and wireless human-machine interaction. *Nano Energy*. 2017;39:328-336.
126. Wang XD, Zhang YF, Zhang XJ, et al. A highly stretchable transparent self-powered triboelectric tactile sensor with metallized nanofibers for wearable electronics. *Adv Mater*. 2018;30(12):1706738.
127. Khandelwal G, Chandrasekhar A, Raj NPMJ, Kim SJ. Metal-organic framework: a novel material for triboelectric nanogenerator-based self-powered sensors and systems. *Adv Energy Mater*. 2019;9(14):1803581.
128. Qian JC, He J, Qian S, et al. A nonmetallic stretchable nylon-modified high performance triboelectric nanogenerator for energy harvesting. *Adv Funct Mater*. 2019;1907414. <https://doi.org/10.1002/adfm.201907414>.
129. Li ZL, Shen JL, Abdalla I, Yu JY, Ding B. Nanofibrous membrane constructed wearable triboelectric nanogenerator for high performance biomechanical energy harvesting. *Nano Energy*. 2017;36:341-348.
130. Cheedarala RK, Duy LC, Ahn KK. Double characteristic BNO-SPI-TENGs for robust contact electrification by vertical contact separation mode through ion and electron charge transfer. *Nano Energy*. 2018;44:430-437.
131. Zhang SL, Lai YC, He X, Liu RY, Zi YL, Wang ZL. Auxetic foam-based contact-mode triboelectric nanogenerator with highly sensitive self-powered strain sensing capabilities to monitor human body movement. *Adv Funct Mater*. 2017;27(25):1606695.
132. Guo HJ, Li T, Cao XT, et al. Self-sterilized flexible single-electrode triboelectric nanogenerator for energy harvesting and dynamic force sensing. *ACS Nano*. 2017;11(1):856-864.

133. Shin SH, Bae YE, Moon HK, et al. Formation of triboelectric series via atomic-level surface functionalization for triboelectric energy harvesting. *ACS Nano*. 2017;11(6):6131-6138.
134. Yao CH, Yin X, Yu YH, Cai ZY, Wang XD. Chemically functionalized natural cellulose materials for effective triboelectric Nanogenerator development. *Adv Funct Mater*. 2017;27(30):1700794.
135. Kim T, Jeon S, Lone S, et al. Versatile nanodot-patterned Gore-Tex fabric for multiple energy harvesting in wearable and aerodynamic nanogenerators. *Nano Energy*. 2018;54:209-217.
136. Bui VT, Zhou QT, Kim JN, et al. Treefrog toe pad-inspired micropatterning for high-power triboelectric nanogenerator. *Adv Funct Mater*. 2019;29(28):1901638.
137. Yu AF, Zhu YX, Wang W, Zhai JY. Progress in triboelectric materials: toward high performance and widespread applications. *Adv Funct Mater*. 2019;29(41):1900098.
138. Kim MP, Lee Y, Hur YH, et al. Molecular structure engineering of dielectric fluorinated polymers for enhanced performances of triboelectric nanogenerators. *Nano Energy*. 2018;53:37-45.
139. Chen BD, Tang W, Jiang T, et al. Three-dimensional ultraflexible triboelectric nanogenerator made by 3D printing. *Nano Energy*. 2018;45:380-389.
140. Ahmed A, Hassan I, Mosa IM, et al. All printable snow-based triboelectric nanogenerator. *Nano Energy*. 2019;60:17-25.
141. Guo HY, Leng Q, He XM, et al. A triboelectric generator based on checker-like interdigital electrodes with a sandwiched PET thin film for harvesting sliding energy in all directions. *Adv Energy Mater*. 2015;5(1):1400790.
142. Wang JH, Wang H, Thakor NV, Lee C. Self-powered direct muscle stimulation using a triboelectric nanogenerator (TENG) integrated with a flexible multiple-channel intramuscular electrode. *ACS Nano*. 2019;13(3):3589-3599.
143. Zhong W, Xu L, Yang XD, et al. Open-book-like triboelectric nanogenerators based on low-frequency roll-swing oscillators for wave energy harvesting. *Nanoscale*. 2019;11(15):7199-7208.
144. Kwak SS, Kim H, Seung W, Kim J, Hinchet R, Kim SW. Fully stretchable textile triboelectric nanogenerator with knitted fabric structures. *ACS Nano*. 2017;11(11):10733-10741.
145. Jao YT, Yang PK, Chiu CM, et al. A textile-based triboelectric nanogenerator with humidity-resistant output characteristic and its applications in self-powered healthcare sensors. *Nano Energy*. 2018;50:513-520.
146. Lai YC, Hsiao YC, Wu HM, Wang ZL. Waterproof fabric-based multifunctional triboelectric nanogenerator for universally harvesting energy from raindrops, wind, and human motions and as self-powered sensors. *Adv Sci*. 2019;6(5):1801883.
147. Ding WB, Wang AC, Wu CS, Guo HY, Wang ZL. Human-machine interfacing enabled by triboelectric nanogenerators and tribotronics. *Adv Mater Technol*. 2019;4(1):1800487.
148. Zhang XS, Han MD, Kim B, Bao JF, Brugger J, Zhang HX. All-in-one self-powered flexible microsystems based on triboelectric nanogenerators. *Nano Energy*. 2018;47:410-426.
149. Li A, Zi Y, Guo H, Wang ZL, Fernández FM. Triboelectric nanogenerators for sensitive nano-coulomb molecular mass spectrometry. *Nat Nanotechnol*. 2017;12(5):481-487.
150. Chen XY, Jiang T, Yao YY, Xu L, Zhao ZF, Wang ZL. Stimulating acrylic elastomers by a triboelectric nanogenerator - toward self-powered electronic skin and artificial muscle. *Adv Funct Mater*. 2016;26(27):4906-4913.
151. Wang LY, Daoud WA. Highly flexible and transparent polyionic-skin triboelectric nanogenerator for biomechanical motion harvesting. *Adv Energy Mater*. 2019;9(5):1803183.
152. Lim GH, Kwak SS, Kwon N, et al. Fully stretchable and highly durable triboelectric nanogenerators based on gold-nanosheet electrodes for self-powered human-motion detection. *Nano Energy*. 2017;42:300-306.
153. Wang XD, Zhang HL, Dong L, et al. Self-powered high-resolution and pressure-sensitive triboelectric sensor matrix for real-time tactile mapping. *Adv Mater*. 2016;28(15):2896-2903.
154. Wang S, Xie GZ, Tai HL, et al. Ultrasensitive flexible self-powered ammonia sensor based on triboelectric nanogenerator at room temperature. *Nano Energy*. 2018;51:231-240.
155. Li SM, Peng WB, Wang J, et al. All-elastomer-based triboelectric nanogenerator as a keyboard cover to harvest typing energy. *ACS Nano*. 2016;10(8):7973-7981.
156. Shian S, Bertoldi K, Clarke DR. Dielectric elastomer based "grippers" for soft robotics. *Adv Mater*. 2015;27(43):6814-6819.
157. Wang X, Yang B, Liu J, Yang C. A transparent and biocompatible single-friction-surface triboelectric and piezoelectric generator and body movement sensor. *J Mater Chem A*. 2017;5(3):1176-1183.
158. Hou C, Chen T, Li Y, et al. A rotational pendulum based electromagnetic/triboelectric hybrid-generator for ultra-low-frequency vibrations aiming at human motion and blue energy applications. *Nano Energy*. 2019;63:103871.
159. Hao C, He J, Zhai C, et al. Two-dimensional triboelectric-electromagnetic hybrid nanogenerator for wave energy harvesting. *Nano Energy*. 2019;58:147-157.
160. Yang H, Yang H, Lai M, et al. Triboelectric and electromagnetic hybrid nanogenerator based on a crankshaft piston system as a multifunctional energy harvesting device. *Adv Mater Technol*. 2019;4(2):1800278.
161. Chen C, Tsai C, Xu M, et al. A fully encapsulated piezoelectric-triboelectric hybrid nanogenerator for energy harvesting from biomechanical and environmental sources. *Express Polym Lett*. 2019;13(6):533-542.
162. Guo Y, Zhang X-S, Wang Y, et al. All-fiber hybrid piezoelectric-enhanced triboelectric nanogenerator for wearable gesture monitoring. *Nano Energy*. 2018;48:152-160.
163. Rodrigues C, Gomes A, Ghosh A, Pereira A, Ventura J. Power-generating footwear based on a triboelectric-electromagnetic-piezoelectric hybrid nanogenerator. *Nano Energy*. 2019;62:660-666.
164. You M-H, Wang X-X, Yan X, et al. A self-powered flexible hybrid piezoelectric-pyroelectric nanogenerator based on non-woven nanofiber membranes. *J Mater Chem A*. 2018;6(8):3500-3509.
165. Seo B, Cha Y, Kim S, Choi W. Rational design for optimizing hybrid thermo-triboelectric generators targeting human activities. *ACS Energy Lett*. 2019;4:2069-2074.

166. Zhu M, Shi Q, He T, et al. Self-powered and self-functional cotton sock using piezoelectric and triboelectric hybrid mechanism for healthcare and sports monitoring. *ACS Nano*. 2019; 13(2):1940-1952.

AUTHOR BIOGRAPHIES



Yiming Liu is a PhD student in the Department of Biomedical Engineering at the City University of Hong Kong since 2018, research assistance in the Department of Architecture and Civil Engineering since 2017. He received his Bachelor degree in Tianjin University in 2015, and his M.Sc. in Hong Kong University of Science and Technology in 2017. His research interests include piezoelectric nanogenerator, triboelectric nanogenerator, flexible electronics, skin-integrated electronics, and wind energy.



Xinge Yu is currently an Assistant Professor of Biomedical Engineering at City University of Hong Kong (CityU). He finished his Ph.D. research of printable flexible electronics at Northwestern University (NU) and University of Electronic Science and Technology of China in 2015. From 2015 to 2018, Xinge Yu was a postdoc. in the Center for Bio-Integrated Electronics at NU and an adjunct

research assistant professor in the Department of Materials Science and Engineering at the University of Illinois at Urbana-Champaign. His research focus on developing skin-integrated electronics and bio-electronics, and conducts multidisciplinary research addressing challenges in practical applications, such as biomedical electronics with compatible physical and chemical properties, and real-time health monitoring.



Prof. Yunlong Zi received his B. Eng. degree from Tsinghua University in 2009. He received his Ph.D. degree from Purdue University in 2014. After his graduate study, he worked as a Postdoctoral Fellow at Georgia Institute of Technology during 2014–2017. Dr. Zi joined the Chinese University of Hong Kong as an Assistant Professor in November 2017, as the founder of the Nano Energy and Smart System laboratory.

How to cite this article: Liu Y, Wang L, Zhao L, Yu X, Zi Y. Recent progress on flexible nanogenerators toward self-powered systems. *InfoMat*. 2020;2:318–340. <https://doi.org/10.1002/inf2.12079>